INFLUENCE OF ANTIMICROBIAL AGENTS ON THE ADHESION OF *Staphylococcus epidermidis* TO BIOMATERIALS

Clara Isabel Teixeira Extremina

Tese submetida à Faculdade de Engenharia do Porto para candidatura à obtenção de grau de Mestre em Engenharia Biomédica

Faculdade de Engenharia
Universidade do Porto
2006

This thesis was supervised by:

Doutor Pedro Lopes Granja
INEB - Instituto de Engenharia Biomédica, Laboratório de Biomateriais

Professor Doutor António Augusto Freitas da Fonseca
Faculdade de Medicina, Universidade do Porto

The host institutions of this thesis were:

INEB - Instituto de Engenharia Biomédica, Laboratório de Biomateriais
Universidade do Porto, Portugal

Faculdade de Medicina da Universidade do Porto
Porto, Portugal

…to Pedro and my Parents

"Just thinking about tomorrow…
and having strength to believe…"

Acknowledgements

This thesis is dedicated to all that made it possible.

Firstly, I would like to express my gratitude and esteem to my supervisors. To Pedro Granja, who maintained his believe and hope in my work with all his enthusiasm and affection besides all the disappointments and difficulties I thank for the patience, availability and all the sincere support.

To Professor Freitas da Fonseca for keeping me on track. I thank for giving me strength and support during this hard journey!

To Professor Mario Barbosa, Director of INEB, for giving me the opportunity to develop my research and for the privilege to work in the Biomaterials Lab.

To António Pedro Fonseca from Faculdade de Medicina do Porto, who follows all my steps in the world of science since my beginning. I thank for the unconditional help and support and for supervising all the periods of this long-term journey. It is a great honour to work with someone who is advisor and mentor…a complete scientist!

I would like to acknowledge to the following persons who contributed to this work:

To Isabel Amaral from INEB, for her kind assistance, support and availability in the Contact Angle equipment.

To Cristina Martins from INEB, for being there with all the affection.

To Manuela Bras from INEB, for the assistance in FTIR.

To Eng. Carlos Sá and Daniela Silva from CEMUP for their assistance in XPS and SEM analyses, respectively.

I am very thankful to all the people from INEB for their kind availability and affection during my work. I would like to specially thanks Inês Gonçalves for the friendship, help and for being there for me, and to Sandra Teixeira for her sympathy, availability and will to help. Thanks to all!

To Paula e Luisa from Lab for their patiente and help in different and important ways!

On a different note, I would like to say to the "noisy little people"… I am still on track!

Finally I would like to thank to my family:

To my Parents…for Life! For presence, comprehension, adaptation abilities, sacrifices write choices in the write times, unconditional help…for all! Without your presence and extreme devotion nothing it was possible!

To my cousins, Joana, Vitor Hugo, João Pedro, Alexandre, António Pedro and Maria João for their smiles and sharing their innocence and fun with me!

To my Grandparents for the experience of life, for the learning in long relevant discussions.

To my "Tia Bela", although not being with us, I still remember her presence and smile! I still know who was "the first king of Portugal"!

To my little friend João Pedro who has travel with me in all my journey and even not knowing what is a Thesis he gives me an unique and special support with his happiness and presence!

To all my Friends, namely to Joana for always being there…!

To Pedro for being everywhere! It is difficult to express my deeply gratitude to someone who gives me the opportunity to Live and to Believe. I would have been lost and hollow without his words and thoughts. This Thesis is yours!

Abstract

Bacterial adhesion and biofilm formation on medical devices frequently leads to difficult-to-treat infections. There are several clinical situations where the inoculation occurs by direct contamination, prior to device insertion, in which bacterial adhesion to polymers occurs under very low shear conditions. The initial step in preventing biomaterials associated infections consists in stopping bacterial adhesion to the device surface. One possible approach relies in the design of antibiotic releasing biomaterials. The aim of the research work described in this thesis was to develop possible modifications on biomaterials, in order to obtain anti adhesive and anti proliferative surface properties, through the sustained release of antimicrobial agents from the surface.

In the present work, silicone, poly(vinyl chloride) (PVC), glass and tissue culture polystyrene were modified with cellulose triacetate (CTA). All materials were incorporated with the antibiotic Imipenem (IMP). CTA membranes were also prepared with the antibiotic entrapped in it. All the materials studied were characterized before and after the modifications in terms of surface morphology by Scanning Electron Microscopy (SEM), surface free energy of interaction by contact angle measurements (quantitative measure of hydrophobicity) and surface structure by Attenuated Total Reflection Fourier Transform Infrared Spectroscopy (ATR-FTIR) and X-ray Photoelectron Spectroscopy (XPS). Antibiotic incorporation and released studies were performed. The *in vitro* adhesion of *Staphylococcus epidermidis* expressing capsular polysaccharide/adhesin (PS/A), the most common etiological agent of colonisation of implantable medical devices, to CTA and to CTA with entrapped IMP (CTA-IMP) was investigated.

All materials tested, after modification with CTA, and including CTA with entrapped IMP, changed their surface hydrophilicity, although not considerable in some cases. ATR-FTIR, along with SEM results, indicated that the CTA coating was not very effective and needs to be improved, although it was out of the scope of the present work to develop a coating technology. However, entrapment of IMP on CTA showed and effective incorporation of the antibiotic, as shown by XPS. Furthermore, the hydrophilicity of CTA was considerably increased by this way. As a consequence, only CTA-IMP was used to subsequent studies of antibiotic release, as well as bacterial

adhesion assays. Release studies showed that this drug-polymer conjugate serves as an adequate reservoir for a sustained release of IMP over an appropriate period of 71h, at an effective bacteriostatic concentration. Moreover, Bacterial adhesion tests showed a statistically significant decrease in the adhesion of *S. epidermidis* RP62A to CTA-IMP when compared to its adhesion to CTA alone. The thermodynamic approach showed a good correlation between free energy of interaction between cells, materials surface and water and bacterial adhesion values.

In conclusion, CTA-IMP is an hydrophilic membrane with enough swelling capacity and elution rate for the incorporation and sustained release of IMP. Therefore the present approach is capable of providing a surface with anti-adhesive and anti-proliferative properties.

Resumo

A adesão bacteriana e a subsequente formação de biofilmes em dispositivos médicos originam frequentemente infecções difíceis de tratar. Existem inúmeras situações clínicas em que a inoculação ocorre por contaminação directa, antes da inserção do dispositivo, nas quais a adesão bacteriana a polímeros pode ser avaliada sob condições de stress reduzido. A etapa inicial na prevenção de infecções associadas a biomateriais consiste em evitar a adesão bacteriana à superficie do dispositivo. Uma possível estratégia consiste no desenvolvimento de biomateriais que libertem antibióticos. O objectivo da investigação descrita nesta Tese foi desenvolver possíveis modificações em biomateriais de forma a obter superfícies com propriedades anti-aderentes e anti-profileralivas, através da libertação sustentada de agentes antimicrobianos a partir da superficie.

No presente trabalho, o silicone, o PVC, o vidro e o poliestireno de culturas celulares foram modificados com triacetato de celulose (CTA). Todos os materiais foram incorporados com o antibiótico Imipenem (IMP). Também foram preparadas membranas de CTA com o antibiótico incorporado. Todos os materiais estudados foram caracterizados antes e depois das modificações em termos de morfologia superficial por Microscopia Electrónica de Varrimento (SEM), de energia livre de interacção através da medição de ângulos de contacto (medida quantitativa de hidrofobicidade) e de estrutura superficial por Espectroscopia de Infravermelhos por Transformada de Fourier com Reflexão Total Atenuada (ATR-FTIR) e Espectroscopia de Fotoelectrões por Raios-X X-ray Photoelectron Spectroscopy (XPS). Foram realizados estudos de incorporação e de libertação do antibiótico. Foi estudada a adesão *in vitro* de *Staphylococcus epidermidis* capsulado PS/A+, o agente mais comum de colonizações em dispositivos médicos implantáveis, ao CTA assim como ao CTA icorporado com IMP (CTA-IMP).

Em todos os materiais ensaiados, depois de modificados com CTA e incluindo o CTA com IMP incorporado, verificou-se uma modificação na hidrofilicidade da superficie, embora não fosse considerável em alguns casos. . Os resultados de ATR-FTRIR juntamente com os de SEM indicaram que o revestimento com CTA não foi tmuito eficiente e necessita de ser melhorado, embora esteja fora do âmbito deste trabalho desenvolver uma tecnologia de revestimento. No entanto, a incorporação de IMP no CTA revelou uma incorporação eficiente do antibiótico, tal como foi demonstrado por

XPS. Para além disso, a hidrofilicidade do CTA foi consideravelmente aumentada desta forma. Como consequência, apenas o CTA-IMP foi usado para estudos posteriores de libertação, bem como de adesão bacteriana. Os ensaios de libertação mostraram que esta conjugação antibiotico-polímero funciona com um reservatório adequado para a libertação continuada de IMP, durante um período apropriado de 71 horas, a uma concentração bacteriostática eficaz de antibiótico. Os estudos da adesão bacteriana revelaram uma diminuição estatisticamente significativa na adesão de *S. epidermidis* RP62A a CTA-IMP em comparação com a adesão a CTA. A abordagem termodinâmica mostrou uma boa correlação entre a energia livre de interação entre a superfície das bactérias, dos materiais e a água e os resultados da adesão bacteriana.

Em conclusão, o CTA-IMP é uma membrana hidrofilica com capacidade de absorção e taxa de eluição suficientes para a incorporação e libertação sustentada de IMP. Consequentemente, é possível obter uma superficie com propriedades anti-adesivas e anti-proliferativas adequadas utilizando a presente estratégia.

Contents

Acknowledgements ..... **iv**

Abstract ..... **vi**

Resumo ..... **viii**

Contents ..... **x**

List of Figures ..... **xiii**

Table List ..... **xv**

Abbreviations ..... **xvi**

1. Introduction **1**

1.1 Relevance and motivation 1

1.2 Objectives 2

1.3 State of the art 2

1.3.1 Microbial adhesion 2

1.3.2 Pathogenesis of biomaterial-centered infections (BCIs) 4

1.3.2.1 *Staphylococcus epidermidis* 5

1.3.3 Consequences of BCI 7

1.3.4 Treatment and prevention of BCI 7

1.3.5 Surface-treatment for drug attachment and incorporation 9

1.3.5.1 Imipenem 13

1.3.6 Cellulose as a biomaterial with biomedical application 15

2. Materials and Methods **17**

2.1 Microorganisms 17

2.1.1 Strains 17

2.1.2 Growth and store conditions 17

2.1.3 Characteristics 17

2.1.3.1 Gram-staining procedure 17

2.1.3.2 Biochemical probes 18

2.1.4 Slime production - Congo red test 18

2.2 Materials and Reagents 19
2.2.1 Antibiotic – Imipenem (IMP) 19
2.2.2 Materials 19
2.2.3 Reagents 19
2.3 Preparation of materials 19
2.3.1 Preparation of cellulose triacetate (CTA) membranes 20
2.3.2 Surface coating of biomedical polymers with CTA 20
2.4 Incorporation of Imipenem on materials 20
2.4.1 Immersion of materials in IMP solution 20
2.4.2 Entrapment of IMP on CTA membranes 21
2.5 Characterization of materials surfaces 21
2.5.1 Structural characterization 21
2.5.1.1 Attenuated Total Reflection - Fourier Transform Infrared spectroscopy (ATR-FTIR) 21
2.5.1.2 X-ray photoelectron spectroscopy (XPS) 22
2.5.2 Surface free energy determination 22
2.5.2.1 Contact angle measurements 22
2.5.2.2 Surface tension determination 23
2.5.3 Surface morphology by Scanning Electron Microscopy (SEM) 25
2.6 Antibiotic incorporation and release 25
2.6.1 Spectrophotometric quantification of IMP 25
2.6.2 IMP incorporation studies 26
2.6.3 IMP release studies 26
2.7 Bacterial adhesion 26
2.7.1 Surface free energy determination between strains, surface adhesion and water 26
2.7.2 Adhesion assay 27
2.7.3 Kirby Bauer test 28
2.8 Statistical analyses 28

3. Results and Discussion 29

3.1 Microorganisms 29
3.1.1 Characteristics 29

3.1.2 Slime production - Congo red test 29
3.2 Characterization of material's surfaces 29
3.2.1 Structural characterization 29
3.2.1.1 Attenuated Total Reflection - Fourier Transform Infrared spectroscopy (ATR - FTIR) 29
3.2.1.2 X-ray photoelectron spectroscopy (XPS) 32
3.2.2 Surface free energy determination 36
3.2.3 Surface morphology by Scanning Electron Microscopy (SEM) 42
3.3 Antibiotic incorporation and release 43
3.3.1 Spectrophotometric quantification of IMP 43
3.3.2 IMP incorporation studies 44
3.3.3 IMP release studies 45
3.4 Bacterial adhesion 47
3.4.1 Surface free energy determination between strains, surface adhesion and water 47
3.4.2 Adhesion assay 48
3.4.3 Kirby Bauer test 50
3.5 Importance of the thermodynamic approach on bacterial adhesion to surfaces 54
3.6 Influence of the surface properties of the materials and bacteria 55

4. Conclusions and Perspectives 56

5. References 57

6. Annexes 68

List of Figures

Figure 1 – Factors involved in the colonization of a plastic biomaterial by *S. epidermidis* (Pascual, 2002) 1

Figure 2 - At separation distances of > 50 nm, only attractive Van der Waals forces occur. At 10 to 20 nm, Van der Waals and repulsive electrostatic interactions influence adhesion. At < 5 nm, short-range interactions can occur, irreversibly binding a bacterium to a surface. From Gottenbos in a adaptation from the original work by Busscher and Weerkamp (Busscher, H.J. and Weerkamp, A.H. 1987) 3

Figure 3 – Electron micrograph of *S. epidermidis*.....6

Figure 4 – Structural formula of Imipenem.....14

Figure 5 – Structural formula of Cilastatin.....14

Figure 6 - Chemical structure of cellulose.....15

Figure 7 – FTIR spectrum of Imipenem.....30

Figura 8 - ATR-FTIR spectrum of silicone (SI) and silicone modified with cellulose triacetate and Imipenem (SI-CTA+IMP) 30

Figure 9 - ATR-FTIR spectrum of cellulose triacetate (CTA) and cellophane (CEL)...31

Figure 10 - ATR-FTIR spectrum of cellulose triacetate (CTA) and cellulose triacetate with Imipenem (CTA-IMP) 32

Figure 11 – Survey spectra of CTA.....33

Figure 12 – Survey spectra of CTA-IMP 33

Figure 13 – C 1s and O 1s peaks of CTA.....34

Figure 14 – C 1s, O 1s and N peaks of CTA-IMP.....34

Figure 15 – Chemical structure of a typical cellulose acetate chain with the hydroxyl groups replaced with acetyl groups.....36

Figura 16 – SEM micrographs of cross-sections of silicone disks: a) unmodified silicone disk, b) silicone disk modified with CTA and IMP.....43

Figure 17 – Imipenem calibration curve.....44

Figure 18 – Concentration of IMP incorporated by the different materials along the time of the experiment.....45

Figure 19 – Concentration of IMP incorporated by CTA-IMP and CEL.....46

Figure 20 - Comparison between adhesion of *S. epidermidis* RP62A and M187-Sn3 to polystyrene.....48

Figure 21 - Comparison between *S. epidermidis* RP62A adhesion to CTA and CTA-IMP.....49

Figure 22 – Bacterial inhibition zone performed by Kirby Bauer test for CTA and CTA-IMP.....50

Figure 23 – SEM micrograph of RP62A strain adhered to a CTA disk.....51

Figure 24 – SEM micrograph of RP62A strain adhered to a CTA-IMP disk.....52

Figure 25 – SEM micrograph of RP62A strain adhered to a CTA disk.....52

Figure 26 – SEM micrograph of RP62A strain adhered to a CTA-IMP disk.....53

Figure 27 - ATR-FTIR spectrum of polystyrene (PS) and modified polystyrene with cellulose triacetate and Imipenem (CDA-IMP).....68

Figure 28 - ATR-FTIR spectrum of PVC and modified PVC with cellulose triacetate and Imipenem (PVC-CTA+IMP).....68

Figure 29 - ATR-FTIR spectrum of glass (GL) and modified glass with cellulose triacetate and Imipenem (GL-CTA+IMP).....69

Table List

Table 1- Surface free energy components at 25 ºC.....23

Table 2- Microbiological characterization of *Staphylococcus epidermidis* strains 29

Table 3- Positions and atomic percentage of species present, obtained by deconvolution of high resolution XPS spectra 35

Table 4- Contact angle ± SD obtained with water, diiodomethane and glycerol for each strain of *S.epidermidis* 36

Table 5- Polar and apolar surface tension parameters of each strain of *S. epidermidis* (mJ/m^2) 37

Table 6- Surface free energy of interaction between bacterial surface and water 37

Table 7- Contact angle ± SD obtained with water, diiodomethane and glycerol for each material 38

Table 8- Polar and apolar surface tension parameters of each material (mJ/m^2).....40

Table 9- Values of the surface free energy of interaction between material's surface and water 41

Table 10- Values of the surface free energy of interaction between a) the materials surface ummodified (CTA) and modified (CTA-IMP), *S. epidermidis* RP62A and water; b) the surface of CTA, water and the *S epidermidis* strains: RP62A and M187-Sn3 47

Abbreviations

BHI.....	Brain Heart infusion
TSA……	Triptic Soy agar
TSB……	Triptic Soy broth
PS/A	Polysaccharide/adhesion
IMP	Imipenem
PS	Polystyrene
GL	Glass
SI	Silicone
PVC	Poly (vinyl chloride)
CTA	Celulose triacetate
CEL	Cellophane
ATR-FTIR	Fourier transform infrared spectroscopy with attenuated total reflectance
XPS	X-ray photoelectron spectroscopy
ΔG^{TOT}_{bwb}	Surface free energy of interaction between bacteria (b) and water (w) (mJ/m^2).
ΔG^{TOT}_{sws}	Free energy of interaction between materials surfaces (s) and water (w) (mJ/m^2)
ΔG^{TOT}_{bws}	Free energy of interaction between materials surfaces (s), bacterial surface (b) and water (w) (mJ/m^2)
ΔG^{AB}_{bwb}	Polar component of the free energy of interaction between bacteria (b) and water (w) (mJ/m^2).
ΔG^{LW}_{bwb}	Apolar component of the free energy of interaction between bacteria (b) and water (w) (mJ/m^2).

ΔG^{AB}_{sws} ..... Polar component of the free energy of interaction between materials surfaces (s) and water (w) (mJ/m^2)

ΔG^{LW}_{sws} ..... Apolar component of the free energy of interaction between materials surfaces (s) and water (w) (mJ/m^2)

ΔG^{AB}_{bws} ..... Polar component of the free energy of interaction between materials surfaces (s), bacterial surface (b) and water (w) (mJ/m^2)

ΔG^{LW}_{bws} ..... Apolar component of the free energy of interaction between materials surfaces (s), bacterial surface (b) and water (w) (mJ/m^2)

γ^{TOT} ..... Surface tension (mJ/m^2)

γ^{LW} ..... Apolar component of surface tension (mJ/m^2)

γ^{AB} ..... Polar component of surface tension (mJ/m^2)

γ^{+} ..... Electron acceptor parameter of the polar component of surface tension (mJ/m^2)

γ^{-} ..... Electron donor parameter of the polar component of surface tension (mJ/m^2)

SEM Scanning electron microscopy

CFU Colony forming unity

MIC Minimal inhibitory concentration

1. Introduction

1.1. Relevance and motivation

There is an increase in the use of biomedical materials in modern medicine, despite some problems resulting from this practice. A major drawback is the biomaterial-centered infections (BCI).

When the biomaterial is implanted the host interacts with it by forming a conditioning film, having an immune response towards the foreign material. The adhesion of microorganisms to the biomaterial surface is mediated by their physico-chemical surface properties and by the properties of the biomaterial surface. After the occurrence of adhesion there is a subsequently growth that can lead to a mature biofilm (Fig. 1).

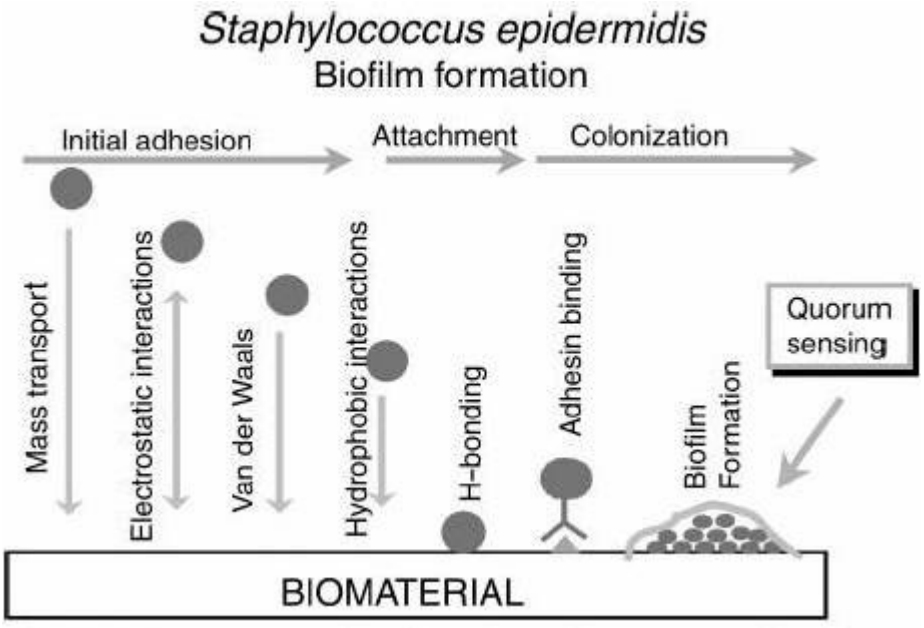

Figure 1 – Factors involved in the colonization of a plastic biomaterial by *S. epidermidis* (Pascual, 2002).

The infection that appears afterwards is difficult to eradicate by antibiotics. Thus, strategies to avoid bacterial adhesion are of utmost importance for a number of clinical applications.

1.2. Objectives

The aim of the research described in this thesis was to develop biomaterial surfaces with anti adhesive and anti proliferative surface properties, through the incorporation and subsequent sustained release of an antimicrobial agent.

1.3. State of the art

1.3.1. Microbial adhesion

Adhesion of micoorganisms begins when they reach the biomaterial surface. This initial step involves specific interactions between bacterial surfaces and specific molecular groups of the substratum (Christensen et al., 1989). Adhesion is mediated by several forces, namely non-specific LW Lifshitz-Van der Waals forces, electrostatic forces, acid-base interactions and Brownian motion forces (Van Oss, 1991).

Over distance smaller than 5 nm there are specific forces that act on localised regions. On the other hand non specific interactions forces have long range properties and involve all the interacting surface as it is illustrated in Fig. 2 (Busscher and Weerkamp, 1987).

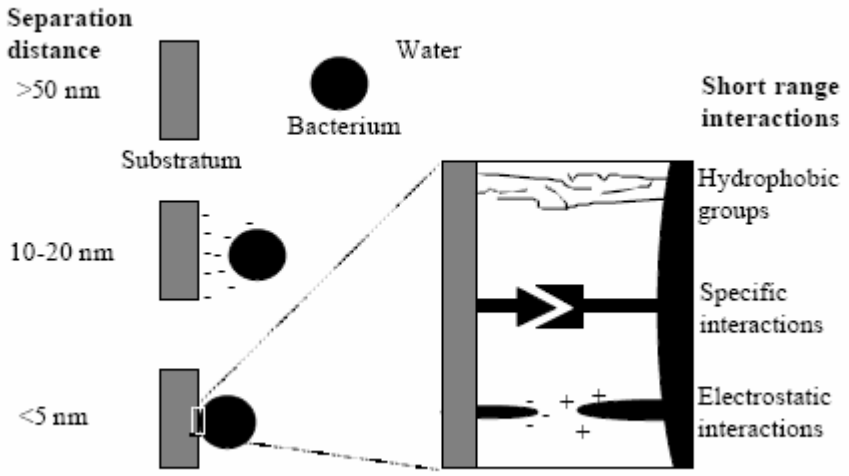

Figure 2 - At separation distances of > 50 nm, only attractive Van der Waals forces occur. At 10 to 20 nm, Van der Waals and repulsive electrostatic interactions influence adhesion. At < 5 nm, short-range interactions can occur, irreversibly binding a bacterium to a surface. From Gottenbos (2001) in an adaptation from the original work by Busscher and Weerkamp (1987).

The attraction of as microorganism to a surface depends on the result of the diferrent non-specific forces, thus physico-chemical surface properties of both microoganisms and surfaces with or without conditioned protein film is of utmost importance in this process. As an example of the influence a conditioning film is albumin which is a strong bacterial adhesion inhibitor (Christensen et al., 1989). Fibronectin and Fibrinogen are proteins that seem to promote adhesion in certain *Staphylococcus epidermidis* strains and the reason for this behaviour is the presence of specific bacterial cell adhesive structures that are directed to these (Christensen et al., 1989; An and Friedman, 1998).

Another important issue is the "false phagocitosis", i.e., biomaterial with bacteria adhered are too large to injust by neutrophils. In fact, Zimmerli and coworkers reported that the activity of phagocytes and polymorphonuclear leukocytes is decreased in the presence of a biomaterial (Zimmerli et al., 1984; Zimmerli et al., 1982). The extraordinary prevalence of slime producing *S. epidermidis* in BCI is explained by the fact that after adhesion to biomaterials most microorganisms start secreting slime and embed themselves in a slime

layer, the glycocalix (Christensen et al., 1989). Slime layer or glycocalix avoid diffusion through it protecting bacteria against host defences (Costerton et al., 1999). The formation of glycocalix gives rise to severe complications, namely the need for implant removal. Nevertheless, the most relevant damage lies in the proliferation of the microorganisms.

1.3.2. Pathogenesis of biomaterial-centered infections (BCIs)

Foreign materials are increasingly used in modern medicine in the case of oncological surgery, replacement surgery or even in the treatment trauma, as constituents of several devices. Sometimes they are used to support or restore human body function, as for example catheters or prosthetic heart valves. As a result of the extended use of these biomaterials there is an increased incidence of BCIs (Gristina, 1987). The degree of incidence of this type of infections varies depending on the type of implant, from hip prosthesis (Dankert et al., 1986) to urinary tract catheters (Denstedt et al., 1998).

Adhesion is the first step towards biofilm formation, which can cause BCI. Severe problems can result, ranging from disfunctioning of the implanted device to lethal sepsis of the patient. Treatment of BCI is complicated as the resistance of microorganisms to antibiotics is higher (Costerton et al., 1999) in a biofilm phenothype than in their planktonic counterparts (Gilbert et al., 1997). As a consequence and when it is possible, the only solution is to remove the infected implant resulting in a considerable increase in costs and patient's suffering. It is thus important to prevent BCI by avoiding bacterial adhesion and biofilm formation.

The routes by which bacteria reach to the surface of intravenous devices have remained constant (Pascual, 2002). Foreign body materials often compromise host, namely by reducing the required inoculum to produce infection. This is the case of the virulent pathogen *Staphylococcus aureus*, which need only of 200 bacteria instead of 10^6 (Elek and Conen, 1957). Furthermore, the most common infecting organism in BCI is not *S. aureus* but *S. epidermidis*, an avirulent specie that normally is not capable of establishing infection (Christensen et al., 1989).

The occurrence of BCI is mainly determined by the possibility of the microorganisms to reach the biomaterial surface. In the case of devices that contact with outside the body

(intravenous catheters, peritoneal dialysis catheters or urinary tract catheters), they are more easily accessible to microorganisms and consequently have a higher incidence of BCI than fully implanted biomaterials (Dankert et al., 1986).

Microorganisms, in several ways at several time points, can reach the biomaterial implant and this is also going to determine the properties of the biomaterial surface they will meet. In the case of airborne microorganisms possibly present in the operating theatre, they can reach the surface before the implantation and interact with a bare substratum surface, not with a conditioning film (Lidwell et al., 1982; Charnley, 1972). Another relevant source of contamination is microorganisms from the skin that can be pushed towards the implant surface. Furthermore, microorganisms can contaminate the operation wound and reach the implant surface through diffusion, active movement or haematogenous transport. The perioperative contamination is believed to be the most common cause of BCI (Ahlberg et al., 1978).

Microorganisms can also reach the implant via the hematogenous route, which can happen at any time after implantation, causing the so-called hematogenous infections. It is interesting to note that the host's microflora is the main source of the infecting organisms, except in the case of airborne microorganisms. The fact that the host is immuno-tolerant for these microorganisms might be seen as an overlooked virulence factor for causing BCI, namely by provide the possibility for the microorganism to survive longer without being attacked by the host's immune system, thus having a bigger chance to reach an implanted biomaterial (Gottenbos, 2001).

1.3.2.1. *Staphylococcus epidermidis*

Staphylococci are gram positive coccus, members of the family *Micrococcaceae*, that produce catalase and can be coagulase positive or negative. The coagulase negative *Staphylococcus* plays an important role in the nosocomial pathogenesis. *S. epidermidis*, being responsible for most of the hospital and foreign body infections, belongs to the natural skin flora.

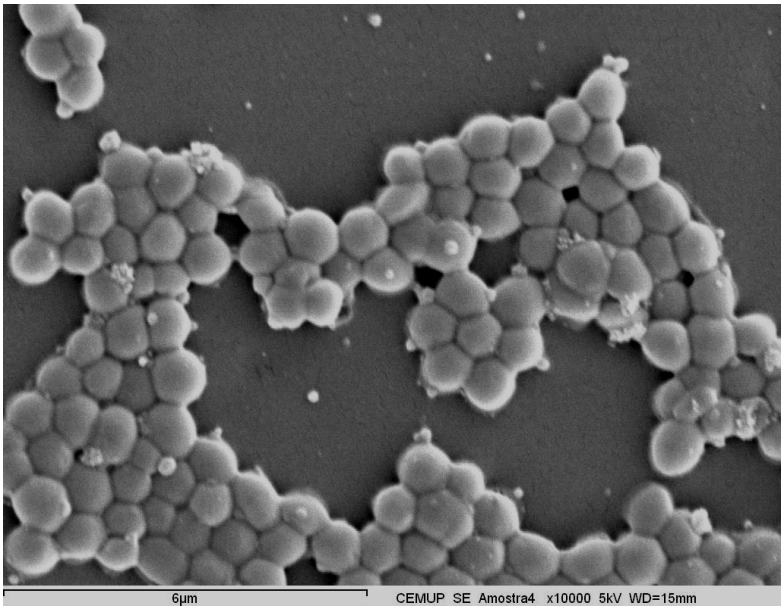

Figure 3 – Electron micrograph of *S. epidermidis*.

A high number of the infections affecting medical devices are associated to *S. epidermidis*, which is therefore called an opportunistic pathogen of foreign bodies (Demirer et al., 2001). It is the most frequent microorganism in intravenous catheter's infections, as it was verified using semi-quantitative techniques (Maki et al., 1977). It is the most frequent microorganism in shunt infections; in a total of 289 hydrocephalic patients, 27 % had developed shunt associated infections, in a period of ten years, being 50 % caused by *S. epidermidis* (Schoenbauem et al., 1975). It is also responsible for prosthetic valves associated endocarditis in more than 40 % of the cases and more than 80 % of these raised infections (Calderwood et al., 1985). *S. epidermidis* is the microorganism that more frequent caused infections of ventriculostomy tubes inserted in patients with cephalic trauma, in order to drain the cephalo-rachidian liquid (LCR) (Mayhall et al., 1982). This microorganism is responsible also for the catheter's infections in patients that received chemotherapy treatment for the neoplasic meningitis. *S. epidermidis* is frequently isolated in more than 50 % of the cases of patients with peritonitis (West et al., 1986). The bacteremia in newborns is associated to catheters infections and to the mechanical ventilation; the majority of the staphylococci coagulase-negative isolated from these children are multiresistant *Staphylococcus epidermidis* (Weinstein et al., 1982).

Furthertmore, it is the most frequent cause of endoftalmia after ocular surgery, mainly in lens implantation (Fisch et al., 1991).

1.3.3. Consequences of BCI

When present at the implant surface microbial biofilms can impair its function or even worsen the clinical state of the patient. As previously pointed out, there are also several examples of non-implanted devices, like urinary tract catheters (Mahieu et al., 1986). These catheters rarely escape colonization by microorganisms causing blockage or, more seriously, bacteriuria (Nickel et al., 1994). Bacteremia, which can cause sepsis and endocarditis, can also often result from urinary tract infections of indwelling catheters. Totally implanted prostheses have lower rates of infections, but present more serious consequences. Infections of vascular grafts and prosthetic valves in the circulatory system yield a high mortality rate (Mayer and Schoenbaum, 1982). Infection of orthopedic implants or mammary prostheses which are deep tissue implants, will usually result in less serious complications although mortalities up to 20% are reported with orthopedic implants (Bengston et al., 1987; Hunter and Dandy, 1977; Fitzgerald and Jones, 1985). In deep implant infections clinical signs are often reported to a year after microbial seeding (Maniloff et al., 1987). In fact, biofilms can stay "silent" for long periods of time and probably without being recognized as part of the infections.

Standard microbiological techniques used to test for the presence of infectious microorganisms do not detect slow growing biofilm organisms. A study by Asaria et al. (1999) reported that clinical signs of infection were only present in 1 out of 5 cases and that 5 of 28 removed scleral explants where biofilm covered. In summary, it seems clear that problems associated with BCI are probably more relevant than generally assumed.

1.3.4. Treatment and prevention of BCI

The minimal inhibitory concentration (MIC; lowest concentration that inhibited visible growth) is significantly lower for planktonic cells than from the sessile cells. As a consequence, the treatment of an established BCI is difficult (Costerton et al. 1999). Since

antibiotics have little or no effect on BCI, the normal procedure is to remove the implant. Afterwards, a new prosthesis is inserted, when the implant site is free of microorganisms, usually 6 months later. For implants in the circulatory system, removal of the implant is dangerous, and a high mortality is associated with these infections. Several treatments are described in the literature to enhance the action of antibiotics towards these biofilm bacteria, namely the ultrasonic treatment (Rediske et al., 1999). Another issue is the application of an electrical field, called the bioelectric effect, is also claimed to enhance the effects of antibiotic treatment (Costerton et al., 1994). These techniques could improve the treatment of BCI with antibiotics.

There is a considerable effort by surgeons to avoid contamination of implants with microorganisms during implantation. Besides better operation hygiene and application of prophylactic antibiotics there are still a significant number of patients suffer from BCIs (Dankert et al., 1986).

In order to avoid the establishment of biofilms in biomaterial surfaces it is necessary to prevent adhesion by reducing the attractive forces between bacteria and biomaterial surface and this can be obtained by optimizing the physico-chemical surface properties of the biomaterial (Everaert et al., 1999). Albumin and heparin coatings have shown to decrease the adhesiveness of biomaterials (Keogh and Eaton, 1994).

The prevention of biofilm formation can also be achieved by avoiding the growth of adhering microorganisms, which can be obtained by application of antimicrobial agents near the biomaterial surface. A possible way is the design of antibiotic releasing biomaterials. Examples are gentamicin-loaded bone cements and silver-loaded catheters (Carlsson et al., 1978; Akiyama and Okamoto, 1979). The problem of this approach is the release of low dose of antibiotics that can be dangerous because of the selection of antibiotic resistant microbial strains (Van de Belt et al., 1999). Even if the antimicrobial agent is covalently bonded onto the biomaterial surface and if it is able to reach the outside of the microbial cells, it can only be employed with antibiotics working at the level of the cell wall or membrane. This seems to be the case of polymers incorporating quaternary ammonium groups (Flemming et al., 2000; Kenawy et al., 1998).

Administering the drugs systemically should be avoided in the case of device-related infections, being the best strategy to locate active agents or drugs only at the surface of the

biomaterial. In fact, systemic administration requires maintaining dose levels throughout the body, which is not the case when using local delivery, where the device surface concentrates the drug at the precise site where it is needed. Systemic administration of high levels of drug should be avoided mainly in patients with diabetes, HIV disease, kidney or liver dysfunction, poor circulation, pregnancy and old age. The amount of drug released must be sufficient and functional to be effective. Another issue is that if there is good drug elution from the device, drug concentration will be high at and near its surface. This effect is easily seen in relatively static environments, such as those of urinary catheters (Zhang et al., 1997).

1.3.5. Surface-treatment for drug attachment and incorporation

The device surface must serve as a reservoir for a large amount of drug and for it to be effective it should be capable of releasing the drug over time in appropriate quantities. The drug must remain functional after sterilization. So, devices incorporating heat-, radiation-, or ethylene oxide-sensitive antibiotics need to be tested for efficacy after sterilization. In order to protect antibiotics from the deleterious effects of sterilization there should be a selection of methods for sequestering drugs on devices.

What is the period of time in hours or days the biomaterial has of sustained high concentrations release? To answer this question, it must consider the short- and long-term effects. There is a period of increased susceptibility to infection that occurs during and immediately after the insertion of a device. If the device is to be in place only during a procedure or perhaps for a few days, then the drug only needs to be available for a few hours or a day or two at most. The longer the device is in place, the greater the probability of infection.

Two longer-term routes of infection are possible, namely the attachment of already internally present bacteria (that exist besides the procedure) onto the surface of the device and transmission of bacteria from external sources via externally communicating devices, such as central venous catheters, drainage tubes and urinary catheters, among others. The proximal end of urinary catheters allows for introduction of bacteria and the device itself as a “vector” acts as a pathway for their migration into the body. The other long-term route is

the occurrence of device-centered infections when there is no external exposure. The high incidence of urinary catheters infection and of vascular and drainage devices that communicate externally suggests that these two longer term pathways of infection normally work together. So, it is clear that an ideal coating with anti infective properties has to elute the antimicrobial as long as possible and at a high concentration, bacteriostatic or even bactericidal. Another important issue is that catheter must be coated on both interior and exterior surface as they can be routes of infection, thus avoiding BCIs.

Modification of device properties by surface treatment has been used in order to decrease the susceptibility to bacterial adhesion and to increase the biocompatibility. The preferential adsorption of protein on hydrophobic poly (perfluroethylene-propylene) surfaces was described as being effective in avoiding bacterial adherence (Hogt et al., 1985). The initial step towards biofilm formation is determined by the hydrophilicity of the surfaces involved (bacterial and biomaterial surface). In fact, an increase in the hydrophilicity of a solid surface decreases the adhesion of various bacterial species. Nevertheless, medical devices are normally made of hydrophobic metals or biomaterials (Shintani, 2004).

In order to modify a hydrophobic surface several techniques are available, such as the hydrogel technology, that involves the use of biocompatible, water-absorbable polymer hydrogels that coat medical-device surfaces (Shintani, 2004). Hydrogels are hydrophilic polymers that can absorb water up to several times their own weight without dissolving, providing thereafter a softer surface for tissue contact. Since most of microorganisms decrease adhesion on hydrogel-coated surfaces because of increased hydrophilicity, hydrogels can be an effective anti-infective coating (Hogt et al., 1985; Hogt et al., 1983; Hogt et al., 1986; Brisset et al., 1996).

Poly (vinyl pyrrolidone) (PVP) and poly (ethylene glycol) (PEG) are examples of hydrogel polymers that have been used in indwelling medical device. Hydrophilic polymer films formed by UV crosslinking derivatives of PVP showed reduction of bacterial adhesion *in vitro* on materials used to construct urinary catheters (Duran et al. 1995). Isla et al. (1996) conclude that the self-assembled monolayer of oligo (ethylene glycol) resists attachment of *S. epidermidis*. Bridgett et al. (1992) found substantial reductions in bacterial adhesion when studied *in vitro* bacterial adherence of *S. epidermidis* on polystyrene surfaces modified by A-B-A copolymers, where A is PEG and B is poly (propylene oxide).

The adhesion process can be altered not only by the surface properties but also by the physiological media and by changing bacterial strains. The modification of the device surfaces in order to increase hydrophilicity may reduce the adherence of some bacterial strains, but may also increase the adherence of some other strains (Hogt et al., 1983).

A chemical barrier against intruding organisms can be obtained by using anti-infective agents that kill microorganisms. Device surfaces with such agents can provide high concentration of anti-infective agents in a local environment, therefore disinfecting bacteria that enter with the medical device or that encounter the device later through any other routes, thus avoiding adhesion and subsequently biofilm formation (Shintani, 2004). The incorporation of non-toxic anti-infective agents, namely antibiotics, antimicrobials or other pharmaceutical agents that kill bacteria on the device's surface could provide another way of avoiding surface colonization. The surface treatments that incorporate anti-adhesive and anti-proliferative agents on the device's surface further provide the possibility of maintaining the material's bulk properties (Shintani, 2004). In the literature, studies describe promising results using coatings that avoid bacterial adhesion besides increasing biocompatibility (Pearson and Abrutyn, 1997).

Current surface-treatment technologies that incorporate anti-infective agents can be classified into, at least, three categories: deposition of a thin film of anti-infective agents on the surface, ionic bonding of anti-infective agents and entrapment of anti-infective agents in a polymer matrix. The direct deposition method applies anti-infective agents directly onto a medical device surface. There are reports of reduction of bacterial adherence in surfaces incorporating silver as well as other antimicrobials. The use of silver is well known, since it is an antibacterial agent with broad-spectrum antimicrobial activity and low toxicity to the human body (Liedberg and Lundeberg, 1989).

The fact that many antibiotic molecules possess either positive or negative charges enables their binding on a medical device surface via ionic bonding. Thereafter it is possible to use surfactants that can interact with both hydrophobic and hydrophilic functional groups. Surfactants are known to inhibit microbial adhesion to hydrocarbons by emulsan (Rosenberg et al., 1983) and to plastics by chlorhexidine gluconate (Tobgi et al., 1987) and Tween 20 (Klotz et al., 1985). The positive or negative charge of the surfactant serve as link for subsequent binding of antibiotics with an opposite charge via ionic binding on the

surfaces of indwelling medical devices. An example of surfactants is Tri dodecyl methyl ammonium chloride, which chemical structure awards a unique ability to, on one hand, bind negatively charged antibiotics via ionic binding on a device surface with antibiotics and, on the other hand, to establish a hydrophobic interaction with a device surface via Van der Walls binding (Shintani, 2004).

In vitro, *in vivo* and clinical studies have shown promising results after entrapment of anti-infective agents in a polymer matrix. It is possible to construct a device or apply a thin layer of coating on a medical device surface using polymer matrices with anti-infective agents (Shintani, 2004). Manufacture of anti-infective polymers presents problems in selecting the anti-infective agents and matrix polymers as well as in finding adequate processes of medical device production. This has met a bigger technical challenge than applying coating technology on devices surfaces (Shintani, 2004).

The technology of non-reactive polymer coatings uses a coating liquid that has specific polymers, anti-infective agents and solvents. When the coating liquid is applied on the medical device surface, solvents evaporate, thus leaving a thin film. This structure consists of polymers with uniform distribution of anti-infective agent and serves as a reserve for a continuous and sustained release over an appropriate period of time, and at an effective concentration. There are no chemical bonds to the matrix polymers but their activity still remains. After release from the matrix, the anti-infective agents can act immediately in a predictable manner in their biological effect. The characteristics of both the anti-infective agents and the polymer matrix influence the performance of prepared anti-infective coatings. When selecting an anti-infective system physiochemical and microbiological properties of both anti-infective agent and polymer should be considered. The application of a device is going to select the choice of anti-infective agents in order to be effective against the major microorganisms that cause infections. When entrapped in the polymer matrix the anti-infective agents must keep their potency, regardless of the broad-spectrum, high bacterial susceptibility, and low toxicity that they should have. For example, after a number of years of application, hypersensitivity reactions to silver sulfadiazine chlorhexidine-coated central venous catheters were reported (Shintani, 2004). The duration of the activity, the efficacy and the toxicity of the coating will be influenced by the loading of the anti-infective agents. The performance of the coating can also be affected by the

solubility of a specific agent, its susceptibility to the targeting microorganisms and its affinity to surrounding tissue. Furthermore, hydrophilicity, as well as the chemical structure of the polymer matrix, plays an important role in the performance of the coating. The polymer matrix in which the anti-infective agent is incorporated is going to select the elution rate of a given anti-infective agent.

Hydrophilic coatings allow water molecules to diffuse easily into the polymer matrix and to diffuse out with anti-infective agents that will kill bacteria in the surrounding area.

In order to release anti-infective agents in a controlled way, coating matrices should be developed with a controllable hydrophilicity. However, in some applications the anti-infective activity still decreases or disappears more rapidly than desired after the device surface contacts with body fluids, thus still allowing bacterial colonization on those devices. This can be explained by the eventual low concentration of the anti-infective agent or by the fact that it is too tightly bonded to the coating to be effectively released.

1.3.5.1. Imipenem

Tienam (imipenem and cilastatin sodium) is a broad spectrum beta-lactam antibiotic and consists of two components: (1) imipenem, the first of a new class of beta-lactam antibiotics, the thienamycins; and (2) cilastatin sodium, a specific enzyme inhibitor that blocks the metabolism of imipenem in the kidney, and substantially increases the concentration of intact imipenem in the urinary tract. Imipenem and cilastatin sodium are present in Tienam in a 1:1 ratio by weight. The thienamycin class of antibiotics, to which imipenem belongs, is characterized by a spectrum of potent bactericidal activity, supposed by broader than that provided by any other antibiotic studied.

Imipenem (N-formimidoylthienamycin monohydrate) is a crystalline derivative of thienamycin, which is produced by *Streptomyces cattleya.* Its chemical name is [5*R*-[5α, 6 α (R*)]]-6-(1-hydroxyethyl) -3-[[2-(iminomethyl) amino] ethyl]thio]-7-oxo-1-azabicyclo [3.2.0] hept-2-ene-2-carboxylic acid monohydrate. It is an off-white, nonhygroscopic crystalline compound with a molecular weight of 317.37. It is sparingly soluble in water and slightly soluble in methanol (http://www.msd-egypt.com). Its empirical formula is $C_{12}H_{17}N_3O_4S \cdot H_2O$, and its structural formula is the following:

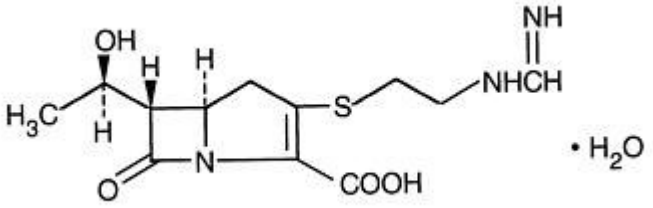

Figure 4 – Structural formula of Imipenem.

Cilastatin sodium is the sodium salt of a derivatized heptenoic acid. Its chemical name is [R-[R*,S*-(Z)]]-7-[(2-amino-2-carboxyethyl)thio]-2-[[(2,2-dimethyl ycloprop yl)carbonyl]amino]-2-heptenoic acid, monosodium salt. It is an off-white to yellowish-white, hygroscopic, amorphous compound with a molecular weight of 380.43. It is very soluble in water and in methanol (http://www.msd-egypt.com). Its empirical formula is $C_{16}H_{25}N_2O_5SNa$, and its structural formula is the following:

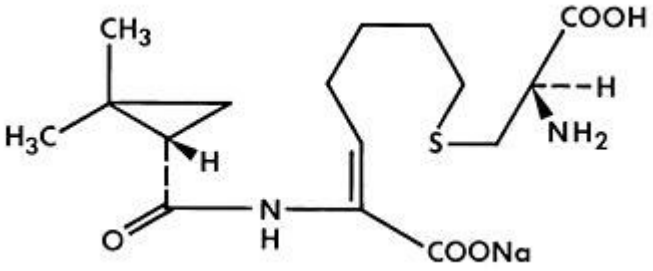

Figure 5 – Structural formula of Cilastatin.

Tienam is a potent inhibitor of bacterial cell wall synthesis and is bactericidal against a broad spectrum of gram-positive and gram-negative, aerobic and anaerobic pathogens. Tienam shares with the newer cephalosporins and penicillins a broad spectrum of activity against gram-negative species, but is unique in retaining the high potency against gram-positive species, previously associated only with earlier narrow-spectrum beta-lactam antibiotics. The spectrum of activity of Tienam includes *Staphylococcus aureus* (Jacqueline et al., 2005), *Staphylococcus epidermidis* (Arciola et al., 2002), *Enterococcus faecalis* (Ono

et al., 2005) and *Bacteroides fragilis* (Aldridge et al., 2003), a diverse group of problem pathogens commonly resistant to other antibiotics.

Tienam is resistant to degradation by bacterial beta-lactamases, which makes it active against a high percentage of organisms such as *Pseudomonas aeruginosa*, *Serratia spp.*, and *Enterobacter spp.*, which are inherently resistant to most beta-lactam antibiotics. Its antibacterial spectrum of Tienam is broader than that of any other antibiotic studied, and includes virtually all clinically significant pathogens.

1.3.6. Cellulose as a biomaterial with biomedical application

Cellulose is a renewable and biodegradable natural polymer, which presents excellent properties to be used as a biomedical material, namely its non-toxicity, high hydrophilicity and some stability to temperature and pH variation. However, cellulose presents low mechanical stability and is susceptible to enzymatic degradation (Granja et al., 1996).

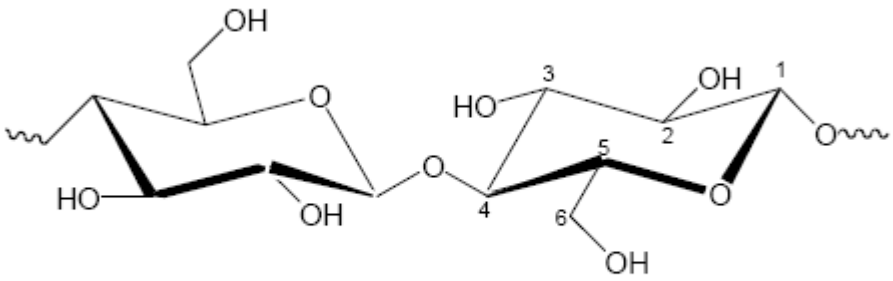

Figure 6 - Chemical structure of cellulose.

Cellulose is a polymer of β-D-glucopyranose unities, presenting a linear structure. All the D-glucose unities in the chain, except an unity in the end, have available hydroxyl groups in carbons 2, 3 and 6, being tri-functional in alcohol groups. These can be subjected to eterification or esterification, resulting in degree of substitution up to 3 (DS = 3) when all the hydroxyl groups are substituted.

In the present work, cellulose acetate film was used. This polymer, when completely acetylated, constitutes the cellulose triacetate (DS = 2.8 - 2.92). Cellulose acetate is frequent used in reverse osmosis, namely for blood purification in hemodialysis (Ishizu, 1991). Kishida et al. (1992) applied polyethylene glycol in cellulose membranes, having verified a reduction in the complement activation, protein and platelet adsorption. Hogt et al. (1983) performed a comparative study on the *in vitro* bacterial adhesion to fluorethylenpropilene (FEP) and cellulose acetate. In this study they verified that the adhesion to cellulose acetate was always reduced comparatively with FEP, having justified this fact with the hydrophilic character of cellulose acetate. Elam et al. (1992) described the use of cellulose derivatives as possible coatings for polytetrafluorethylene (PTFE). In this study the authors used ehtylhydroxiethylcellulose (EHEC), having described low reactions in tissues near the biomaterial. Elam et al. (1993), in another study described the adsorption of EHEC in polyurethane and PTFE, where they found a significant decrease in fibronectin, vitronectin and fibrinogen adsorption. Although there was significant decrease in complement activation, protein adsorption or platelet adhesion no bacterial adhesion studies were described. Okada et al., (1997) described phosphorylated cotton with incorporated ions silver as an adequate substract to avoid bacterial adhesion. Fonseca et al (2001) reported that the chemical modification of cellulose acetate by both deacetylation and phosphorylation decreased bacterial adhesion. Cooksey (2005) described methods for coating low-density polyethylene film or barrier films with methyl cellulose; there was a significant reduction in the adhesion of *Listeria monocytogenes*.

2. Materials and Methods

2.1. Microorganisms

2.1.1. Strains

The strain *Staphylococcus epidermidis* ATCC 35984 (RP62A) was kindly provided by American Type Culture Collection (ATCC) and the strain M187-Sn3 was a generous gift from Gerald B. Pier (Channing Laboratory, Harvard Medical School, Boston, MA, EUA). The strain RP62A is capsulated and is positive (PS/A+). The strain M187-Sn3 is an isogenic mutant of M187, polysaccharide/adhesion negative (PS/A-). Each mutant strain contains a single copy of the 13.6-kb transposable unit *Tn*917LTV1 incorporated into the wild-type parent genome at a unique site (Muller et al., 1993). This insertion results in cessation of the expression of PS/A and slime (Sn3). The strain ATCC 35984/RP62A was used as a control for hydrophobicity studies.

2.1.2. Growth and store condititions

Bacteria were stored at –70 °C in Brain Heart Infusion (BHI) medium (Merck, USA) containing 20 % glycerol. (Christensen et al., 1995).
S. epidermidis (RP62A and M187-Sn3) were routinely grown at 37°C on Triptic Soy agar (TSA Difco, USA) or Triptic Soy Broth (TSB, Difco, USA) (Bridgett et al., 1992; Rad et al., 1998; Vacheethasanee et al., 1998).

2.1.3. Characteristics

2.1.3.1. Gram-staining procedure

The bacteria were mounted and fixed on a slide before staining. The entire slide was completely covered with crystal violet for about 60 seconds. Afterwards this it was flood with iodine solution that was standing for a minute as well. The slide was rinsed with water for 5 seconds and decolorized using 95% ethyl alcohol. The slide was then

stained with safranin for 30 seconds. The slide was finally rinsed with water and dried at room temperature. All the slides were observed at the optical microscope.

2.1.3.2. Biochemical probes

Catalase: The breakdown of hydrogen peroxide into oxygen and water is mediated by the enzyme catalase. When a small amount of an organism that produces catalase is introduced into hydrogen peroxide, rapid elaboration of bubbles of oxygen, the gaseous product of the enzyme's activity is produced. First it was used an inoculating loop to transfer a small amount of the colony to be tested (pure culture colonies), from the agar to the surface of a clean, dry glass slide. Then is was placed immediately one drop of 3% hydrogen peroxide on to the organism on the slide. The slide was observed for immediate formation of bubbles indicating oxygen production.

Coagulase: The staphylococcal enzyme coagulase will cause inoculated citrated rabbit plasma to gel or coagulate. Coagulase converts soluble fibrinogen in the plasma into insoluble fibrin that can be easily visualized. First one drop drop of rabbit plasma is added to a glass slide and then several colonies in the rabbit plasma were emulsified. If the test is positive immediate clumping is observed, but if is negative no clumping is observed.

2.1.4. Slime production - Congo red test

The medium was prepared with 37 g BHI broth, 50 g of sucrose, 10 g of agar and 0.8 g of Congo red. Congo red stain was prepared as a concentrated aqueous solution, autoclaved at 121 ºC for 15 min and then added to the other components of the culture medium after cooling to 55 ºC. Plates were inoculated with one or more colonies of the original isolate and incubated at 37 ºC for 24 h. A result was considered positive when black colonies grew on the surface. Strains that did not produce slime developed red colonies (Freeman et al., 1989).

2.2. Materials e Reagents

2.2.1. Antibiotic – Imipenem (IMP)

The antibiotic used in this study was Imipenem (Tienam; Merck Sharp & Dohme), a specific antibiotic indicated for the treatment of Gram-positive bacteria infections.

2.2.2. Materials

The materials used in this study were polystyrene (Tissue culture, Starstedt), glass (Marienfeld), silicone (SI; Statice Santé), polyvinyl chloride (PVC; Mallinckrodt Hi-Lo^{TM}), cellulose triacetate (CTA, Eastman Chemical Company) and cellophane (CEL; Hexabio).

For the modification of materials and for the adhesion assays, sheets of silicone (SI; thickness = 1mm) and cellophane (CEL; thickness = 0,1 mm) were cut in a pneumatic bore maker to obtain disks with a diameter of 12 mm.

The disks of PVC were obtained from Mallinckrodt Hi-Lo^{TM} endotracheal tubes. The PVC tubes were split and cut into pieces of 5 cm and then heated below the melting point of PVC, between two glass microscope slides, for 20 s at 180 ºC. All experiments were performed on flattened Mallinckrodt^{TM} PVC substrates (Balazs et al., 2004).

2.2.3. Reagents

All the reagents were of analytical grade and used without further purification.

2.3. Preparation of materials

All the disks used in this study were previously sonicated for 15 min with 0.1% (v/v) Tween 80 in an ultrasonic cleaner (Branson, USA, 45kHz), (Christensen et al., 1995) and for 15 min with distilled water. Then all the disks were immersed in distilled water for 24 h and incubated in a vacuum woven at 30ºC.

2.3.1. Preparation of cellulose triacetate (CTA) membranes

In a first approach CTA was dissolved in acetone to form a 4 % solution. Films were casted onto glass dishes. A 7 ml polymer solution was poured into each dish (diameter = 90 mm) and the dish was then heated in an incubator at 40 ºC. Thin films were obtained after evaporation of the solvent and used for further investigation after 24 h.

Preliminary assays with the CTA membranes prepared with acetone were not satisfactory because This solvent has a rapid evaporation and the membranes had been with high porosity and rugosity. As a consequence CTA was dissolved in chloroform-methanol (9:1 vol-%) mixture to form a 2% solution (Bhat and Wavhal, 2000). Films were casted onto glass dishes. A 7 ml polymer solution was poured into each dish (diameter = 90 mm) and the dish was then heated in an incubator at 20º C. After evaporation of the solvent thin films were obtained and used for further investigation after 24 h.

2.3.2. Surface coating of biomedical polymers with CTA

A solution of CTA dissolved in acetone was prepared to form a 4% solution. The solution was used for further investigation after 24h. Silicone, polystyrene, glass and PVC disks were immersed for 24h at room temperature in the 4 % CTA solution.

2.4. Incorporation of Imipenem on materials

2.4.1. Immersion of materials in IMP solution

All the disks of all the materials studied (unmodified polymers, polymers coated with CTA and CTA membranes) were immersed in a solution of IMP (512 µg/ml) for 24 h at room temperature. After modification of the surfaces all the disks were dried in the vacuum woven at 20 ºC for 24 h.

2.4.2. Entrapment of IMP on CTA membranes

In order to improve the incorporation of IMP, it was decided to entrap the antibiotic on the membrane. For that, the CTA and IMP powders were mixed and then dissolved in chloroform-methanol (9:1 vol %) mixture to form a 2% solution of CTA (Bhat and Wavhal, 2000) with a concentration of Imipenem of 512 µg/mll. Films were casted onto glass dishes. A 7 ml polymer solution was poured into each Petri dish (diameter = 90 mm) and the dish was then heated in an incubator at 20º C. After evaporation of the solvent thin films were obtained and used for further investigation after 24 h.

2.5. Characterization of material's surfaces

2.5.1. Structural characterization

2.5.1.1. Fourier transform infrared spectroscopy with attenuated total reflectance (ATR-FT-IR)

The Infrared spectra were recorded with a FTIR system 2000 from Perkin-Elmer, using the SplitPea^{TM} accessory (Harrick Scientific), provided with a silicon internal reflection element and configured for external reflectance mode. The disks were previously dried at 20ºC in a vacuum woven for 24 h. The spectra were obtained from a 200 µm diameter sampling area, after accumulation of 200 interferograms, at a 4 cm^{-1} spectral resolution. All spectra were corrected for the ATR characteristic progressive increase in the absorbance at lower wave numbers, using the software equipment. Peak identification was obtained from the correspondent second-derivative spectra in the range between 3900 and 400 cm^{-1}. Hundred scans were acquired.

The Imipenem was analysed by FT-IR spectroscopy, using the KBr technique. Each pellet was prepared by blending 2 mg of antibiotic powder with 100 mg of KBr, previously dried at 105ºC for 24 h. The Infrared spectra were immediately recorded in the FT-IR system previously described, by accumulation of 200 interferograms, at a 4 cm^{-1} spectral resolution.

2.5.1.2. X-ray photoelectron spectroscopy (XPS)

Spectra were obtained on a VG Scientific ESCALAB 200 A, using a Mg Kα X-ray radiation as the excitation source (15 kV), operated at 300 W. The analyzer was run in the constant analyzer transmission mode. The emitted photoelectrons were analyzed at a 55º take-off angle from the horizontal surface plane, for all analyses. Survey spectra were acquired over a binding energy range of 0 to 1100 eV, using a pass energy of 50 eV. High-resolution spectra for the C1s, O1s and N1s regions were obtained, using a pass energy of 20 eV. Two samples were analyzed: one with antibiotic and one without antibiotic. The charging correction was made according to the aromatic carbon using the binding energy of 285.0 eV. The deconvolution of the high resolution spectra was made by means of a least-squares peak analysis software, XPSPEAK version 4.1, using the Gaussian/Lorenzian sum function.

Element atomic percentages were calculated from the integrated intensities of the XPS peaks, taking into account the atomic sensitivity factors of the instrument data system.

2.5.2. Surface free energy determination

2.5.2.1. Contact angle measurements

The contact angle measurements were performed using a video-based optical contact angle measurement device OCA 15 plus, provided with an electronic syringe unit (Dataphysics, Germany). Distilled and deionized water, with conductivity lower than 1 µS/cm, diiodomethane (> 99%, Sigma-Aldrich) and glycerol (> 99.8%, Sigma-Aldrich), were used. The surface tension of the liquids was determined by the pendent drop method. Measurements were carried out at 25ºC, inside a thermostatted environmental chamber, previously saturated with a pool of the liquid sample. The liquid densities at 25ºC were determined using a density meter (Anton Paar, Germany). The polar and dispersive components of the surface tension of the liquids at 25ºC were estimated from the correspondent values at 20ºC, obtained from the literature. (Della Volpe and Siboni, 1997) The estimation was based on the assumption that the ratio between the dispersive and the polar components of the surface tension did not vary with the temperature. Static contact angles were measured at 25ºC by the sessile drop method, using droplets of 4 µL for water, 1 µL for diiodomethane and 4 µL for glycerol . Due to the swelling

nature of the membranes and to the eventual reorientation of surface groups, (Andrade JD et al., 1985) time-dependent measurements were taken for a period of 100 s, and the experimental contact angles extrapolated to time zero. A minimum of 5 drops were made per sample type in at least three different samples. Contact angles, surface tensions and surface free energies were calculated by SCA20 software (Dataphysics, version 2.0), fitting the drop profiles to the Young-Laplace equation. The polar and dispersive contributions of the surface energies were calculated according to the method of Owens and Wendt (1969).

2.5.2.2. Surface tension determination

After obtaining the contact angle values for water, diiodomethane and glycerol, and with the values of Table 1, it can be applied the Young-Laplace equation and the surface tensions of materials can be calculated using software SCA20 (Dataphysics, verrsion 2.0).

Table 1 - Surface free energy components at 25 ºC.

	Tensão superficial (mJ/m^2)			
Liquid	γ_l^{TOT}	γ_l^{LW}	γ_l^{+}	γ_l^{-}
Water	71.52	21.418	25.053	25.053
Diiodomethane	50.46	50.46	0	0
Glycerol	64.33	34.18	3.94	57.696

The values of $\sqrt{\gamma_s^+}$ and $\sqrt{\gamma_s^-}$ are obtained, which allow us to calculate γ_s^{AB} from the equation:

$$\gamma_s^{AB} = 2\sqrt{\gamma_s^+ \times \gamma_s^-} \qquad \text{eq. (1)}$$

Finally, the surface tension value can be obtained for the material surface γ_s^{TOT} and for the bacteria surface γ_b^{TOT}, according to eq. (2):

$$\gamma_s^{TOT} = \gamma_s^{AB} + \gamma_s^{LW} \text{ and } \gamma_b^{TOT} = \gamma_b^{AB} + \gamma_b^{LW} \quad \text{eq. (2)}$$

The total free energy of interaction between the molecules from material's surface is calculated by the polar and apolar components of the free energy of interaction, ΔG_{sws}^{LW} and ΔG_{sws}^{AB}, respectively (van Oss et al., 1987):

$$\Delta G_{sws}^{TOT} = \Delta G_{sws}^{LW} + \Delta G_{sws}^{AB} \quad \text{eq. (3)}$$

the apolar component is determined by equation 4:

$$\Delta G_{sws}^{LW} = -2\left(\sqrt{\gamma_s^{LW}} - \sqrt{\gamma_w^{LW}}\right) \quad \text{eq. (4)}$$

in which γ_s^{LW} and γ_w^{LW} represent the apolar components of the surface tension for surface and water, respectively.

The polar component ΔG_{sws}^{AB} is related to the individual surface tension components by:

$$\Delta G_{sws}^{AB} = -2\gamma_{bw}^{AB} \quad \text{eq. (5)}$$

where,

$$\gamma_{bw}^{AB} = 2\left(\sqrt{\gamma_b^+\gamma_b^-} + \sqrt{\gamma_w^+\gamma_w^-} - \sqrt{\gamma_b^+\gamma_w^-} - \sqrt{\gamma_b^-\gamma_w^+}\right) \quad \text{eq. (6)}$$

for what:

$$\Delta G_{sws}^{AB} = -4\left(\sqrt{\gamma_s^+\gamma_s^-} + \sqrt{\gamma_w^-\gamma_w^+} - \sqrt{\gamma_s^+\gamma_w^-} - \sqrt{\gamma_s^-\gamma_w^+}\right) \quad \text{eq. (7)}$$

The total free energy of interaction is given by:

$$\Delta G_{sws}^{TOT} = \Delta G_{sws}^{AB} + \Delta G_{sws}^{LW}$$

2.5.3. Surface morphology by Scanning Electron Microscopy (SEM)

The surface morphology of the disks was examined by scanning electron microscopy (SEM), with a scanning electron microscope JEOL, model JSM –6301F, Noran Instruments), in CEMUP. The samples were sputtered-coated with gold (JEOL JFC 1100).

2.6. Antibiotic incorporation and release

2.6.1. Spectrophotometric quantification of IMP

UV spectroscopy was used to measure the amount of IMP adsorbed onto the different biomaterials studied. The materials used in this study were tested to evaluate their ability to adsorb and release IMP.

The adsorption kinetics of a drug onto a material's surface is generally a complex issue. In order to study the adsorption kinetics of IMP, it was necessary to assess the content of IMP present either on the material's surface or remaining in solution. The method consisted in measuring the absorbance of IMP in solution by UV spectroscopy. A calibration curve was firstly obtained and its use restricted to the linear part, which followed Beer's law (equation 8), so that the concentration of IMP in solution could be determined from the absorbance obtained by UV spectroscopy.

$$A=acl \qquad \text{eq. (8)}$$

Where A is the absorbance, c the concentration, a is a proportionality constant related to the solution being tested (known as absorptivity) and l is the pathlength, which is constant, and in this case equal to 1 (Thomas and Ando, 1996)

The adsorption of IMP was studied in saline solution. An UV spectrum of this solution was drawn, from 200 to 1100 nm, in order to determine the absorbance peak. A calibration curve according to Beer-Lambert law was obtained so that the concentration of antibiotic in solution could be determined. For each concentration three samples were collected.

2.6.2. IMP incorporation studies

CTA membranes prepared with acetone (section 2.3.1) and the disks cellophane were immersed in an antibiotic solution (512 µg/ml) during 24h. Samples were removed throughout the 24h of incorporation and measured via UV spectroscopy at 298 nm. The flasks used for the incorporation studies were used as control and thus their incorporation of IMP was taken into consideration. When the concentrations were too high, solutions were diluted in other to fit the straight line in the calibration curve. Each assay was performed in triplicate.

2.6.3. IMP release studies

After the incorporation of the antibiotic (512 µg/ml) the CTA and CEL disks were immersed in a saline solution during 330 min in order to detect the concentration of IMP released by the disks. Samples were collected throughout the time of study and measured using UV spectroscopy at 298 nm.

The CTA-IMP membranes were immersed in a saline solution for 4260 min (71h) in order to release the antibiotic adsorbed. Samples were collected throughout the time of study and measured using UV spectroscopy at 298 nm. Each assay was performed in triplicate.

2.7. Bacterial adhesion

2.7.1. Surface free energy determination between strains, surface adhesion and water

The study of the energy interaction between two surfaces that are immersed in water is given by the interfacial tensions LW and AB.

The polar energy of interaction is given by equation 9:

$$\Delta G_{bws}^{AB} = \gamma_{bw}^{AB} - \gamma_{bs}^{AB} - \gamma_{ws}^{AB} \qquad \text{eq. (9)}$$

Using equations 5 and 6 and knowing that:

$$\gamma_{bw}^{AB} = \gamma_{b}^{AB} + \gamma_{w}^{AB} + \gamma_{bw}^{AB}, \qquad \text{eq.(10)}$$

then

$$\Delta G_{bws}^{AB} = 2\left[\begin{array}{l}\left(\sqrt{\gamma_b^+} - \sqrt{\gamma_s^+}\right).\left(\sqrt{\gamma_b^-} - \sqrt{\gamma_s^-}\right) - \left(\sqrt{\gamma_b^+} - \sqrt{\gamma_w^+}\right).\\ \left(\sqrt{\gamma_b^-} - \sqrt{\gamma_w^-}\right) - \left(\sqrt{\gamma_s^+} - \sqrt{\gamma_w^+}\right).\left(\sqrt{\gamma_s^-} - \sqrt{\gamma_w^-}\right)\end{array}\right] \qquad \text{eq.(11)}$$

In order to obtain the total free energy of interaction it should be added the ΔG_{bws}^{LW}:

$$\Delta G_{bws}^{LW} = -2\left(\sqrt{\gamma_b^{LW}} - \sqrt{\gamma_w^{LW}}\right)\left(\sqrt{\gamma_s^{LW}} - \sqrt{\gamma_w^{LW}}\right) \qquad \text{eq.(12)}$$

so that,

$$\Delta G_{bws}^{TOT} = \Delta G_{bws}^{LW} + \Delta G_{bws}^{AB} \qquad \text{eq.(13)}$$

2.7.2. Adhesion assay

In the adhesion assay the strains RP62A and M187-Sn3 were incubated in 10 ml of TSB inoculated with bacteria grown on TSA plates not older than 2 days, and grown for 18±2 h at 37 ºC at 150 rpm. Afterwards, 1 ml of each cell suspension was transferred to 150 ml of fresh TSB, which was incubated for 18±2 h at 37 ºC at 150 rpm. The protocol developed by Fonseca et al. (2004) for the adhesion assay was modified and adapted. Bacteria were washed twice in saline solution (0.9% NaCl prepared in distilled water), by centrifugation for 15 min at 1000 g, and resuspended in PBS in a standard inoculum corresponding to approximately 10^8 cfu/ml. This inoculum concentration was

determined by making serial dilutions in saline solution and performing colony counts in duplicate on TSA plates after overnight incubation.

The CTA and CTA-IMP disks were placed in 24-well polystyrene microtitre plates. One millilitre of the bacteria inoculum was added to the wells of sterile microtitre plates with or without disks. Negative controls were obtained by placing the disks in a saline solution without bacterial cells and the sterile controls were obtained by placing the disks in fresh TSB medium without bacterial suspension. The plates were incubated for 2 h at 37 ºC. After incubation, microtitre plates were then carefully rinsed twice with saline solution to remove non-adherent bacteria for bacterial quantification. Plates were then air-dried, a solution of 0.1% safranin (Gross et al., 2001) was added for 60 s and the wells were rinsed again to remove excess dye. The bound dye was extracted using acetone/ethanol and the Optical Density (OD) was measured at 492 nm, in order to detect the safranin, using a micro-ELISA plate reader (O'Toole et al., 1999). Each assay was performed in triplicate and repeated three times.

2.7.3. Kirby Bauer test

The antibacterial activity of the unmodified material (CTA, prepared as described in section 2.3.1) and of the modified material (CTA-IMP, prepared as described in section 2.4.2) was assessed *in vitro* by a modified Kirby Bauer test. To this aim, the disks were placed in Petri plates containing Muller-Hinton agar (MH, Difco, USA), seeded with 10^8 cfu/ml (0.5 McFarland) of *S. epidermidis* RP62A. After incubation at 37 ºC for 18 h, the bacterial growth inhibition zone around the disks was analyzed (Donelli et al., 2002).

2.8. Statistical analyses

All the assays were compared using oneway analysis of variance (ANOVA) by applying Levene's test of homogeneity of variances, the Tukey multiple-comparisons test, and the paired samples *t*-test using SPSS software (Statistical Package for the Social Sciences). The difference was considered statistically significant for $P \leq 0.05$.

3. Results and Discussion

3.1. Microorganisms

3.1.1. Characteristics

Table 2 shows that all the strains studied were Gram positive, coagulase negative and catalase positive, as expected for *S. epidermidis*.

Table 2 - Microbiological characterization of *Staphylococcus epidermidis* strains.

***Staphylococcus epidermidis* strains**	**Gram staining**	**Coagulase**	**Catalase**
RP62A	+	-	+
M187-Sn3	+	-	+

3.1.2. Slime production - Congo red test

The colonies of RP62A were black centered (PS/A, slime positive) and of M187-Sn3 were red (PS/A, slime negative).

3.2. Characterization of materials surfaces

3.2.1. Structural characterization

3.2.1.1. Attenuated Total Reflection – Fourier Transform Infrared spectroscopy (ATR – FTIR)

To survey the peaks corresponding to the antibiotic studied, this was analysed by FTIR spectroscopy, using the KBr technique (Fig. 7).

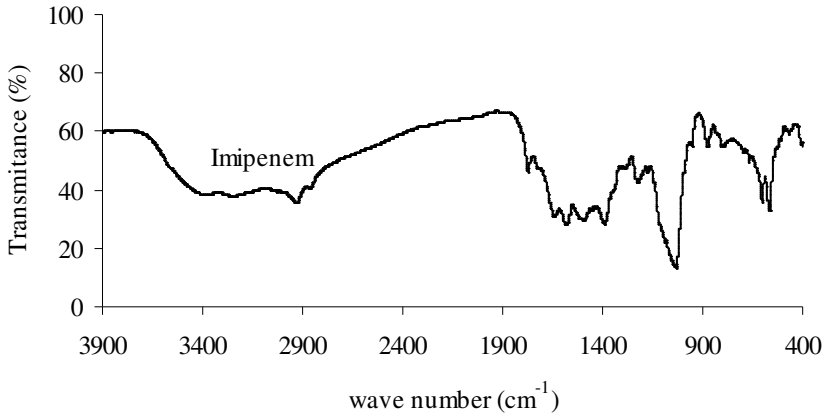

Figure 7 – FTIR spectrum of Imipenem.

Fig. 8 shows the characteristic spectrum of unmodified silicone, in comparison with the modified material (SI-CTA+IMP). Using this technique, no detectable changes were observed as a result of any of the treatments performed. The film is probably not thick enough to be detected by the ATR-FTIR analyses. Also, it is likely that the adhesion between the CTA coating and the silicone substrate was not effective. The spectrum obtained for unmodified silicone is similar to those reported in the literature (Fonseca, 1999)

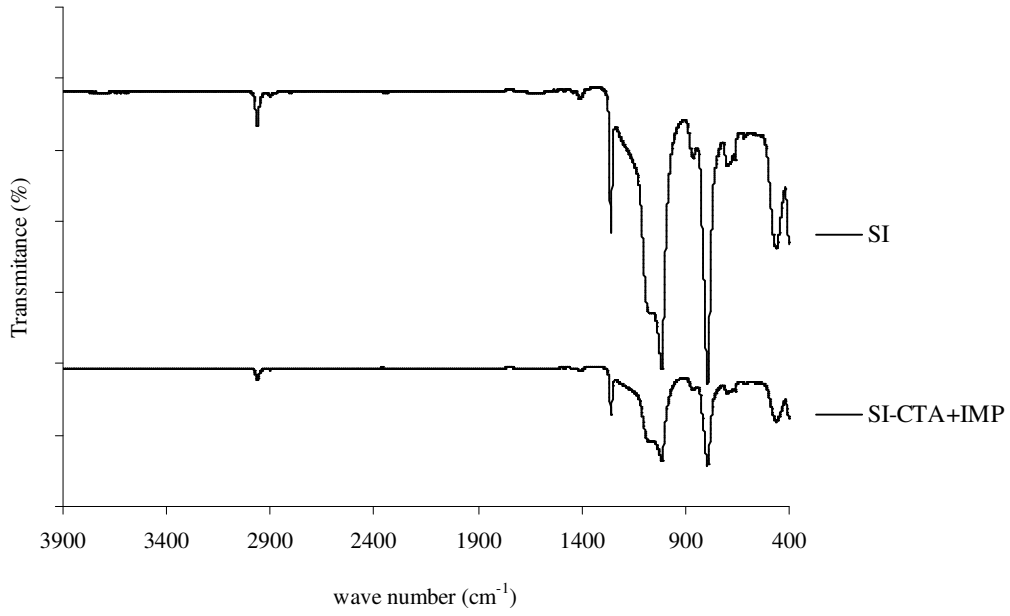

Figura 8 - ATR-FTIR spectrum of silicone (SI) and silicone modified with cellulose triacetate and Imipenem (SI-CTA+IMP).

In the Annex, the ATR-FTIR spectra for the other materials tested are available (Figs. 27-29). These materials showed the same behaviour as silicone, presenting no detectable changes in structure between the uncoated and coated materials. Similarly to what observed in the case of silicone, probably the adhesion between the CTA film and these substrates was poor.

Fig. 9 shows the ATR-FTIR spectrum of cellulose triacetate membranes prepared with acetone, and cellophane disks without any treatment. The analyses were carried out to assess the differences between acetylated (CTA) and deacetylated (CEL) cellulose.

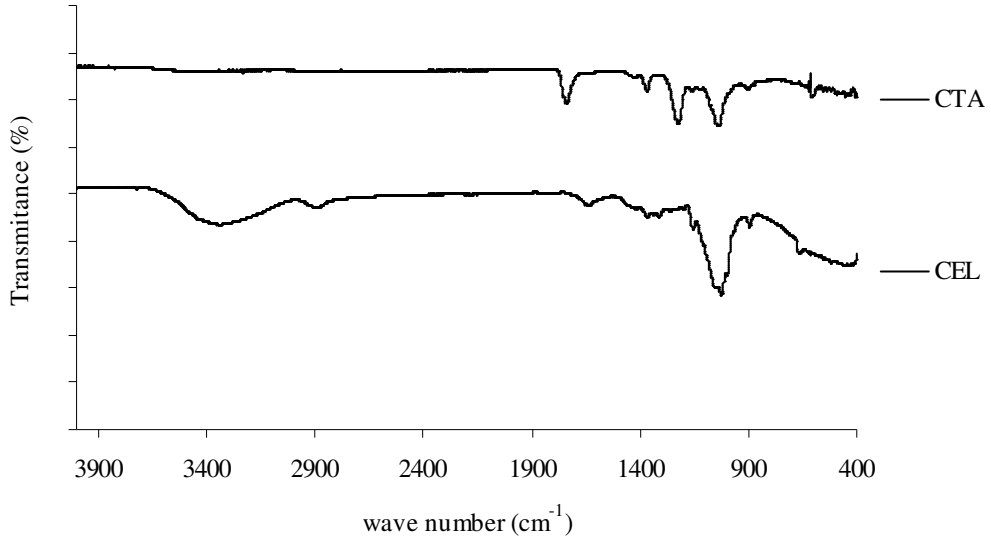

Figure 9 - ATR-FTIR spectra of cellulose triacetate (CTA) and cellophane (CEL).

In comparison with CTA (Fig. 9) the ATR-FITR spectrum of CEL showed a reduction of the peak at 1720 cm^{-1}, generally assigned to carbonyl functionalities in acetate groups (Klem et al., 1998).

Although it was possible to prepare the CTA films in acetone they were not adequate for use in further assays, namely due to their high porosity and surface roughness. For these reasons another method of preparing CTA was tested, by dissolving CTA in chloroform-methanol, as previously described in Bhat and Wavhal (2000). Fig. 10 represents the ATR-FTIR spectrum of cellulose triacetate membranes prepared with chloroform-methanol, as well as these membranes prepared with entrapped IMP.

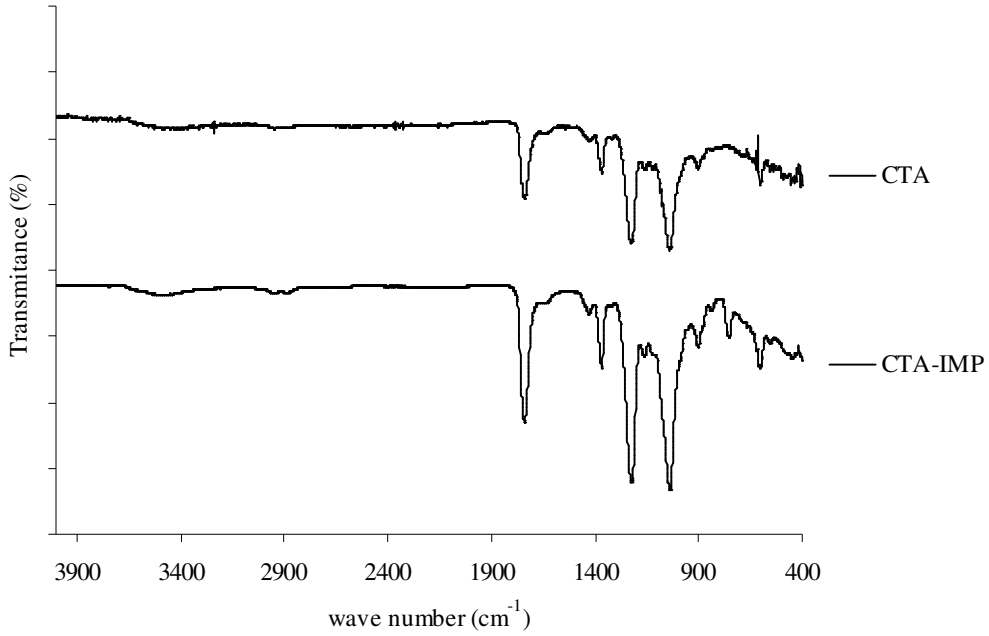

Figure 10 - ATR-FTIR spectrum of cellulose triacetate (CTA) and cellulose triacetate with Imipenem (CTA-IMP).

In the case of CTA-IMP membranes, no detectable changes were observed by ATR-FTIR between the material without antibiotic and the material prepared with antibiotic, probably because this is not a surface modification since the antibiotic is incorporated in the bulk of the material. Hence, in order to detect the presence of the antibiotic in the CTA membranes the XPS technique was used.

3.2.1.2. X-ray photoelectron spectroscopy (XPS)

The materials analysed by XPS were CTA membranes prepared with or without IMP (using the chloroform-methanol method). The objective was to detect nitrogen compounds on the membrane with IMP. The survey spectrum of CTA (Fig. 11) shows that C and O were present in the film, and that there is no contamination. The spectrum is similar to typical XPS spectra obtained for CTA (Beamson and Briggs. 1992). The expected C (1s) and O (1s) peaks were observed in the CTA samples examined (Fig. 13). The atomic percentage of carbon and oxygen obtained by high resolution XPS spectra were 65.05 % of C and 34.95 % of O for the CTA sample (Table 3).

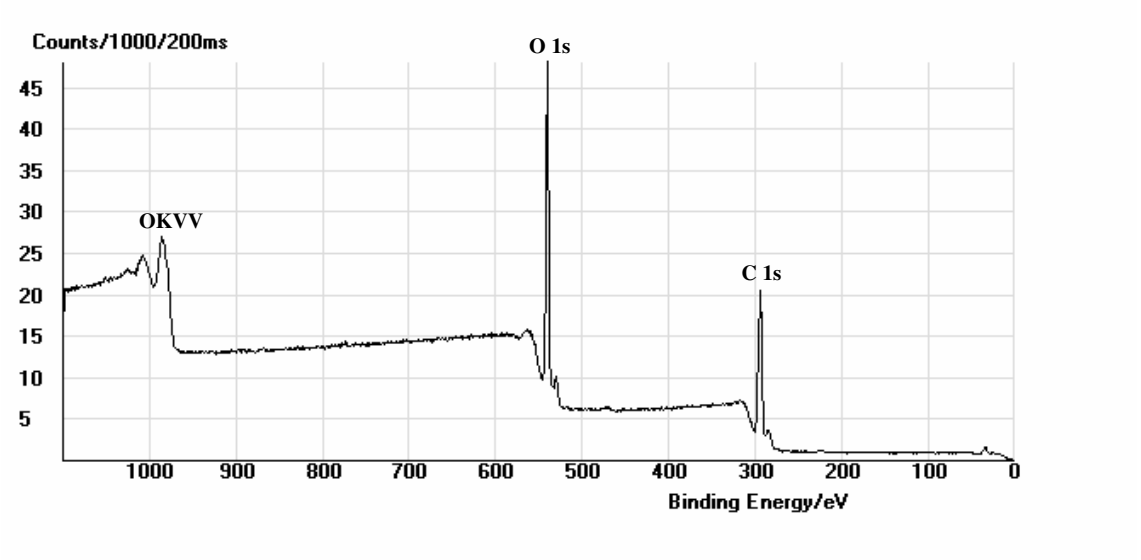

Figure 11 – XPS survey spectra of CTA.

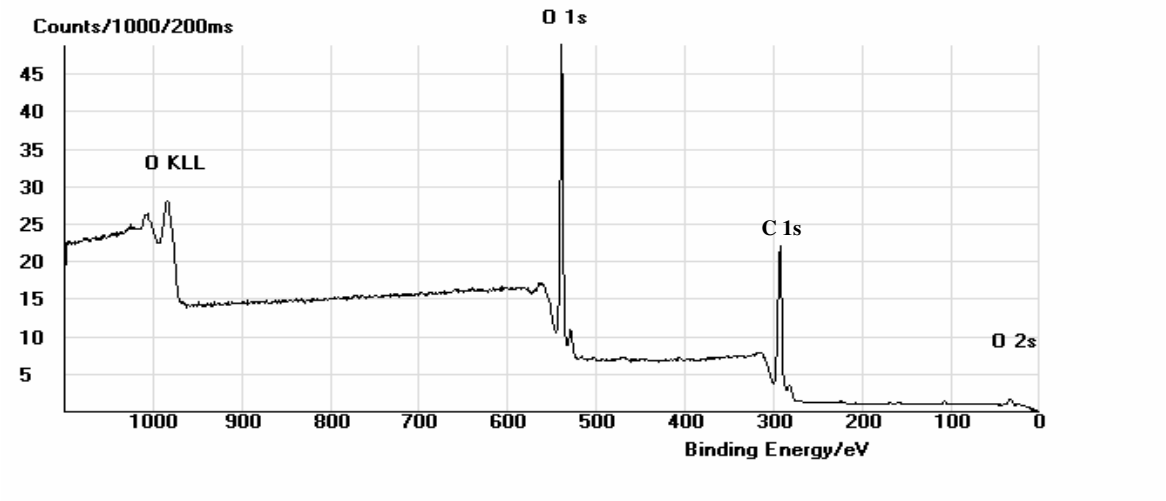

Figure 12 – XPS survey spectra of CTA-IMP.

In the case of CTA-IMP membranes the atomic percentage of carbon, oxygen and nitrogen obtained by high resolution XPS spectra were 66.8 %, 32.7 % and 0.4 %, respectively (Figs. 12 and 14 and Table 3).

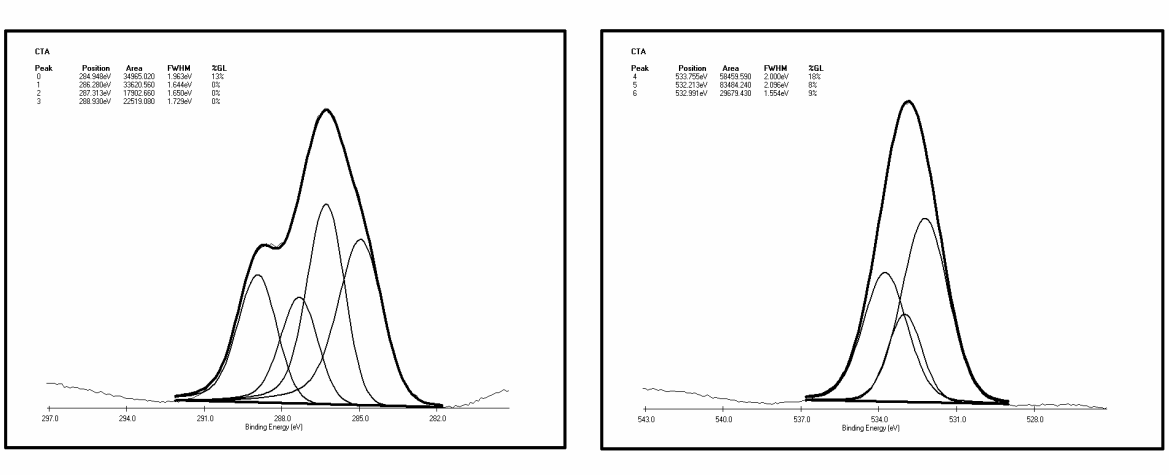

Figure 13 – C 1s and O 1s peaks of CTA.

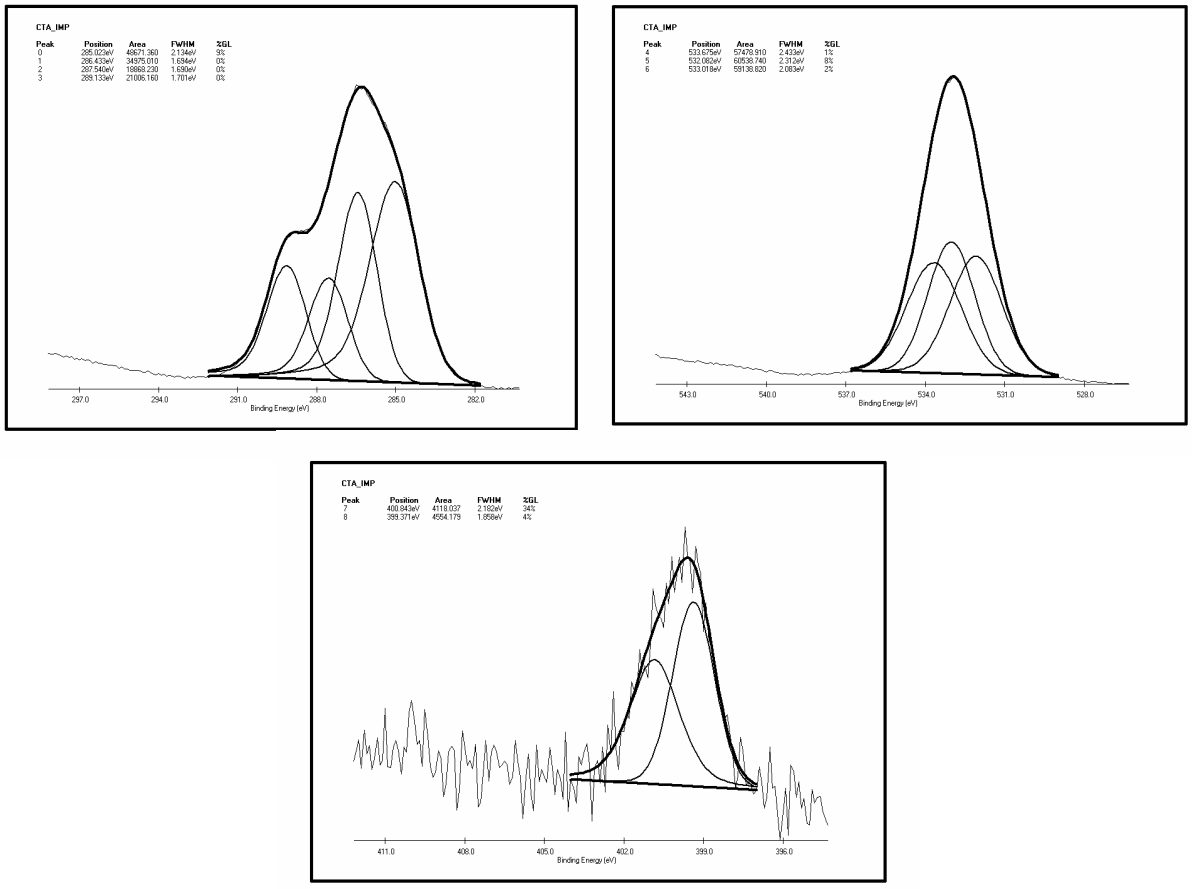

Figure 14 – C 1s, O 1s and N peaks of CTA-IMP.

The components of C 1s spectrum and O 1s spectrum are available in the literature (Beamson and Briggs. 1992). Their respective positions in comparison with the experimental values obtained can be seen in Table 3.

Table 3 – Positions and atomic percentage of species present, obtained by deconvolution of high resolution XPS spectra.

	Peak	**CTA (Binding energy)**		**C TA-IMP (Binding energy)**
		Position observed (atomic %)	**Position expected**	**Position observed (atomic %)**
C 1s	1	284.95 (32.08%)	285.40	285.02 (39.40%)
	2	286.28 (30.84%)	286.63	286.43 (28.32%)
	3	287.31 (16.42%)	287.98	287.54 (15.28%)
	4	288.93 (20.66%)	289.22	289.13 (17.01%)
O 1s	1	533.76 (34.06%)	533.68	533.68 (32.45%)
	2	532.21 (48.64%)	532.27	532.08 (34.17%)
	3	532.99 (17.29%)	533.08	533.02 (33.38%)
N	1	---	400.3	400.84 (47.49%)
	2	---	399.8	399.37 (52.51%)

The peaks found in the literature for the components of N spectrum correspond to NH_2 (peak 2) and NH (peak 1) (Beamson and Briggs, 1992). Since no significant shifts occurred in the peak's positions, there is no evidence of any chemical interaction between CTA and IMP.

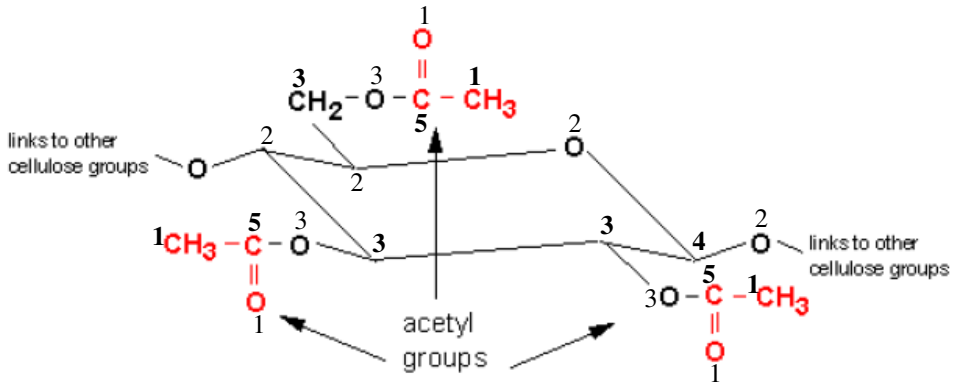

Figure 15 – Chemical structure of a typical cellulose acetate chain with the hydroxyl groups replaced with acetyl groups. The numbers in bold correspond to the peaks of C 1s spectrum and the other numbers to the peaks of O 1s spectrum.

3.2.2. Surface free energy determination

Table 4 shows the contact angle values reported in the literature (Fonseca, 2001) for the different strains assayed with three different liquids, two polar (water and glycerol) and one apolar (diiodomethane).

Table 4 – Contact angle values reported (Fonseca, 2001) with water, diiodomethane and glycerol for the different strains of *S. epidermidis* used in this study.

Strain	**θ Water (º)**	**θ Diiodomethane (º)**	**θ Glycerol (º)**
RP62A	23.1 ± 2.1	64.5 ± 2.4	24.2 ± 2.8
M187-Sn3	42.8 ± 3.1	50.2 ± 1.8	56.9 ± 2.5

P≤0.05.

On the basis of the contact angle values for the three liquids and the data from Table 1, the values of the apolar component or Lifshitz-van der Waals (LW) and of the electron acceptor (γ^+) and electron donor (γ^-) components of the surface tension were obtained (Fonseca et al., 2001). Table 5 shows the surface tensions obtained for each strain.

Table 5 – Polar and apolar surface tension parameters of each strain of *S. epidermidis* (mJ/m^2).

Strain	γ^{LW} (mJ/m^2)	γ^{+}(mJ/m^2)	γ^{-} (mJ/m^2)	γ^{AB} (mJ/m^2)	γ^{TOT} (mJ/m^2)
RP62A	25.8	6.1	42.8	32.3	58.1
M187-Sn3	33.9	0.1	44.7	4.2	38.1

Table 5 shows that the surface tension for the capsulate strain PS/A+ (RP62A) is higher than the non capsulated strain (M187-Sn3). This difference is mainly associated with the absence of the polissacaridic capsule in strain M187-Sn3, therefore increasing its basic character.

On the basis of the polar and apolar surface tension components of each strain the polar and apolar components of the surface free energy of interaction between bacterial surface and water were determined (Table 6).

Table 6 – Surface free energy of interaction between bacterial surface and water.

Strain	ΔG_{bw}^{LW} (mJ/m^2)	ΔG_{bw}^{AB} (mJ/m^2)	ΔG_{bw}^{TOT} (mJ/m^2)
ATCC35984(RP62A)	-0.4	15.5	15.1
M187-Sn3	-2.9	31.5	28.6

The value of the surface free energy of interaction between bacterial surface and water (ΔG_{bw}^{TOT}) constitutes a quantitative measure of the hydrophobicity of the bacterial surface. Therefore, the non-capsulated strain M187-Sn3 showed a ΔG_{bw}^{TOT} value more positive than the capsulated strain RP62A, which indicates higher hydrophilicity. These results are in accordance with previous findings (Fonseca, 1999).

Table 7 shows the contact angles of the different materials assayed with three different liquids, two polar (water and glycerol) and one apolar (diiodomethane).

Table 7 - Contact angle ± SD obtained with water, diiodomethane and glycerol for each material.

Material	θ_{water} (º)	$\theta_{diiodomethane}$ (º)	$\theta_{glycerol}$ (º)
CTA	64.5 ± 3.4	42.9 ± 4.0	70.7 ± 3.5
CTA-IMP	53.6 ± 3.8	44.3 ± 2.8	72.3 ± 3.6
PS	42.2 ± 1.7	42.2 ± 1.6	65.0 ± 1.8
PS-CTA	62.8 ± 0.8	28.7 ± 1.2	71.0 ± 1.3
PS-IMP	45.8 ± 2.6	60.4 ± 2.3	67.5 ± 1.2
PS-CTA+IMP	74.8 ± 1.7	32.2 ± 1.8	71.6 ± 2.6
PVC	90.8 ± 1.1	29.7 ± 1.9	81.2 ± 0.8
PVC-CTA	83.1 ± 1.1	24.2 ± 0.8	82.1 ± 1.8
PVC-IMP	81.7 ± 0.5	26.9 ± 2.5	80.4 ± 1.0
PVC-CTA+IMP	72.6 ± 0.3	38.9 ± 2.4	73.4 ± 1.7
SI	119.9 ± 1.1	85.9 ± 0.7	111.8 ± 2.1
SI-CTA	115.9 ± 1.4	76.5 ± 1.8	115.3 ± 0.2
SI-IMP	118.0 ± 1.2	84.0 ± 2.0	114.2 ± 0.6
SI-CTA+IMP	114.9 ± 0.8	100.4 ± 2.3	117.0 ± 1.1
GL	63.4 ± 2.2	64.1 ± 1.3	95.1 ± 1.5
GL-CTA	31.2 ± 1.3	46.6 ± 1.1	66.5 ± 1.0
GL-IMP	56.2 ± 1.4	52.9 ± 1.6	66.3 ± 1.1
GL-CTA+IMP	59.6 ± 1.2	50.2 ± 0.3	63.1 ± 0.4

$P<0.05$

CTA - cellulose triacetate; PS - polystyrene; PVC – poly(vinyl chloride); SI - silicone; GL - glass; IMP - Imipenem.

In Table 7 it can be observed that the water contact angles of the unmodified materials decrease in this order: SI > PVC > CTA > GL > PS. After coating with CTA it was expected that the water contact angle would decrease or increase to a value near the one for CTA (64.5º). The water contact angle of PS-CTA (62.8º) increased to almost the same value of CTA, but for the other materials, the water contact angle decreased only slightly (approximately 4º for SI, 8º for PVC). In the case of glass it decreased considerably from 63.4 to 32º. When IMP was incorporated it can be observed that the water contact angle also only slightly changed in comparison with the unmodifidied materials (-2º for SI, -9º for PVC, -7º for GL and +4ª for PS), but were kept close to the

contact angle values of the materials coated with CTA in the cases of PVC and SI. When the materials were coated with CTA and incorporated with IMP, the water contact angle also slightly decreased in almost all the materials tested (5º for SI, 18º for PVC and 3º for GL) and usually differed very little comparing to the behaviour observed after incorporation of IMP alone. In the case of PS-CTA+IMP an increase of 33º was observed when compared with the unmodified material, which is consistent with the increase observed after coating with CTA. The entrapment of IMP in CTA membranes promoted a considerable decrease in the water contact angle of about 11º. Water contact values thus indicate that the coating with CTA was more effective in the hydrophilic (PS and GL) than in the hydrophobic materials (PVC and SI).

Results from Table 7 reveal that the measurement of contact angles using only one liquid (water) provide only limited information between modified and unmodified surfaces. Therefore, two other liquids were used (diiodomethane and glycerol) in order to detect possible AB interactions and to further elucidate differences between the tested surfaces. The contact angle values for the three liquids allowed determining the values of the apolar or Lifshitz-van der Waals (LW) component, and the electron acceptor (γ^+) and electron donor (γ^-) components of the surface tension (Table 8).

On the basis of the polar and apolar surface tension components of each material the polar and apolar components of the surface free energy of interaction between materials' surface and water were determined (Table 9).

Table 8 - Polar and apolar surface tension parameters of each material tested (mJ/m^2).

Material	γ^{LW} (mJ/m^2)	γ^{+} (mJ/m^2)	γ^{-} (mJ/m^2)	γ^{AB} (mJ/m^2)	γ^{TOT} (mJ/m^2)
CTA	36.5	0.0	20.4	0.0	36.5
CTA-IMP	37.0	0.0	44.0	0.0	37.0
PS	35.8	0.0	44.9	0.0	35.8
PS-CTA	44.3	0.0	25.8	0.0	44.3
PS-IMP	27.7	0.0	52.1	0.0	27.7
PS-CTA+IMP	41.7	0.0	8.7	0.0	41.7
PVC	43.9	0.0	2.3	0.0	43.9
PVC-CTA	45.9	0.0	8.3	0.0	45.9
PVC-IMP	45.0	0.0	8.8	0.0	45.0
PVC-CTA+IMP	38.3	0.0	11.7	0.0	38.3
SI	13.6	0.0	0.0	0.0	13.6
SI-CTA	19.1	0.0	1.5	0.0	19.1
SI-IMP	15.3	0.0	0.8	0.0	15.3
SI-CTA+IMP	7.8	0.0	2.1	0.0	7.8
GL	25.9	0.0	59.0	0.0	25.9
GL-CTA	35.7	0.0	74.7	0.0	35.7
GL-IMP	32.4	0.0	33.9	0.0	32.4
GL-CTA+IMP	33.9	0.1	25.2	3.2	37.1

Table 9 - Values of the surface free energy of interaction between material's surface and water.

Material	ΔG_{sw}^{LW} (mJ/m^2)	ΔG_{sw}^{AB} (mJ/m^2)	ΔG_{sw}^{TOT} (mJ/m^2)
CTA	-3.97	-9.74	-13.71
CTA-IMP	-4.23	32.56	28.40
PS	-3.66	34.00	30.34
PS-CTA	-8.21	1.42	-6.78
PS-IMP	-0.80	44.26	43.46
PS-CTA+IMP	-6.68	-41.23	-47.90
PVC	-7.96	-69.91	-77.88
PVC-CTA	-9.23	-42.43	-51.66
PVC-IMP	-8.62	-40.85	-49.48
PVC-CTA+IMP	-4.87	-31.61	-36.48
SI	-1.75	-100.21	-101.96
SI-CTA	-0.14	-75.45	-75.58
SI-IMP	-1.02	-82.08	-83.10
SI-CTA+IMP	-6.80	-71.34	-78.14
GL	-0.43	53.60	53.17
GL-CTA	-3.65	72.83	69.18
GL-IMP	-2.28	16.36	14.08
GL-CTA+IMP	-2.87	0.35	-2.52

The value of the surface free energy of interaction between material surface and water (ΔG_{sw}^{TOT}) constitutes a quantitative measure of the hydrophobicity of the material. Table 8 shows that the unmodified materials are monopolar with basic character (GL > PS > CTA > PVC), except SI that is apolar. These data are in accordance with the data from Table 9, in which glass is presents a $\Delta G_{sw}^{TOT} > 0$, followed by PS, which means that these materials have affinity with water, i.e., they are hydrophilic. On the contrary, CTA, PVC and SI present ΔG_{sw}^{TOT} values gradually more negative. This fact evidences the hydrophobic character of these materials. It can be observed that when the γ^- decreases, the surface free energy of interaction between the surface and water also decreases.

Table 8 shows that the apolar SI changes to monopolar with basic character when coated with CTA or incorporated with IMP or even becomes more basic with CTA+IMP (increases 2.1 mJ/m^2). PVC presents a similar behaviour to SI, increasing the γ^- component (10 mJ/m^2). The surface free energy of interaction of these materials decreases with the coating of the material with CTA, which means that the materials become less hydrophobic. GL and PS are the ones with higher γ^- values and when modified with CTA+IMP the values for this polar component decrease (54 mJ/m^2 for GL and 36 mJ/m^2 for PS). Therefore, it is expected that with a decrease in γ^- values the surface free energy of interaction also decreases. Data from Table 9 show that GL-CTA+IMP and PS-CTA+IMP have a $\Delta G_{sw}^{TOT} < 0$, which means these materials changed from hydrophilic to hydrophobic. CTA-IMP presents higher polar component values in comparison with CTA, which can be due to a substitution of two acetate groups for the antibiotic components, imipenem and cilastatin, leaving four hydroxyl groups free, and thus increasing the acidic character of the membrane.

The hydrophobic materials (SI, PVC and CTA) when coated with CTA (except CTA itself), IMP and CTA+IMP decreased in hydrophobicity or even became hydrophilic, in the case of CTA. For the hydrophilic materials the hydrophilicity increased with the incorporation of IMP but decreased when the materials were coated with CTA and incorporated with IMP.

It is of major interest to coat hydrophobic materials like SI or PVC, to modify their surface properties, due to their good mechanical properties. However, due to limitation in scope and timeframe of the present work, only CTA-IMP was used in further studies of antibiotic incorporation and release, and in bacterial adhesion studies.

3.2.3. Surface morphology by Scanning Electron Microscopy (SEM)

Fig. 16 shows the cross-section of an uncoated (a) silicone disk and one coated (b) with CTA. The artefacts in the figure are due the technique of sample preparation.

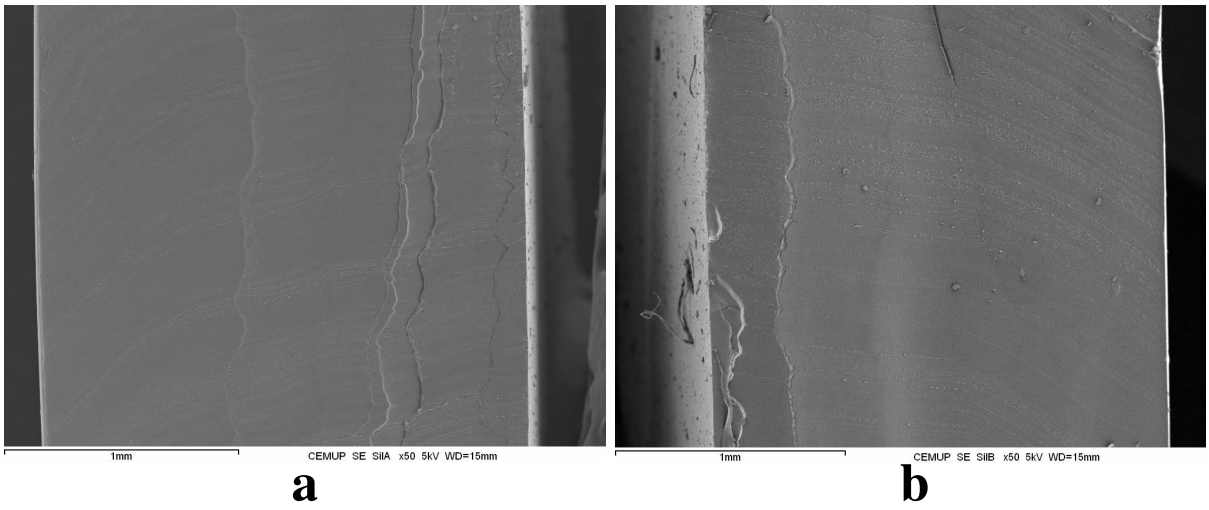

Figura 16 – SEM micrographs of cross-sections of silicone disks: a) unmodified silicone disk, b) silicone disk modified with CTA and IMP.

Fig. 16 shows no differences between uncoated and coated silicone. Similar findings were obtained when observing the other materials, which is in agreement with previous structural analyses, which indicated that the coating with CTA, using the present methodology, has not been effective especially using the hydrophobic substrates (silicone and poly(vinyl chloride)). Several improvements could be carried out to enhance the effectiveness of the coating procedure, such as the surface modification of the substrates (Ratner, 1993). However, such modifications leading to an effective coating were out of the scope of the present work, mainly due to time limitations. Hence, subsequent studies were pursued with the coating material (CTA) with entrapped IMP, in order to evaluate its ability to incorporate and adequately release the antibiotic, and thus prevent bacterial adhesion.

3.3. Antibiotic incorporation and release

3.3.1. Spectrophotometric quantification of IMP

The adsorption of Imipenem was investigated in saline solution. An UV spectrum of this solution was drawn, from 200 to 1100 nm, in order to determine the absorbance

peak, which was found to occur at 298nm. The results were fit of the linear part of the curve (Fig. 17), which is described by the equation

$$A = 0.0134c + 0.0178 \qquad \text{eq. (14)}$$

A correlation factor of 0.9791 was found. All the concentration results were based on this calibration curve.

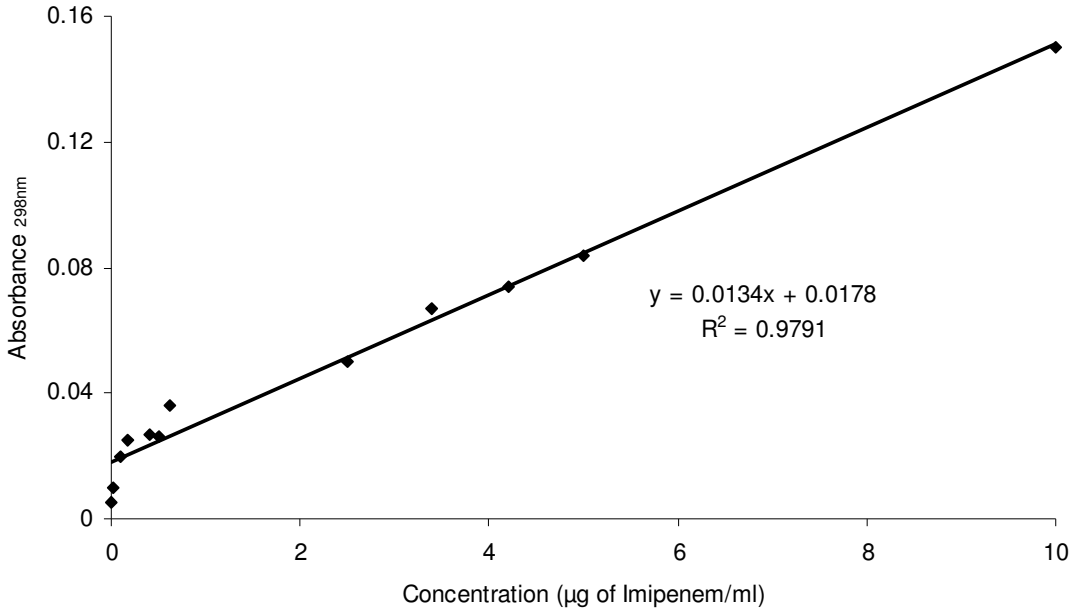

Figure 17 – Imipenem calibration curve.

3.3.2. IMP incorporation studies

Samples were removed throughout the time of incorporation (1440 min) and measured using UV spectroscopy at 298 nm in order to assess the concentration of IMP incorporated by the disks of CTA and CEL. Cellophane was used to assess the differences between acetylated (CTA) and fully deacetylated (CEL) cellulose. When the concentrations were too high, solutions were diluted in order to fit the straight line in the calibration curve (eq. 14).

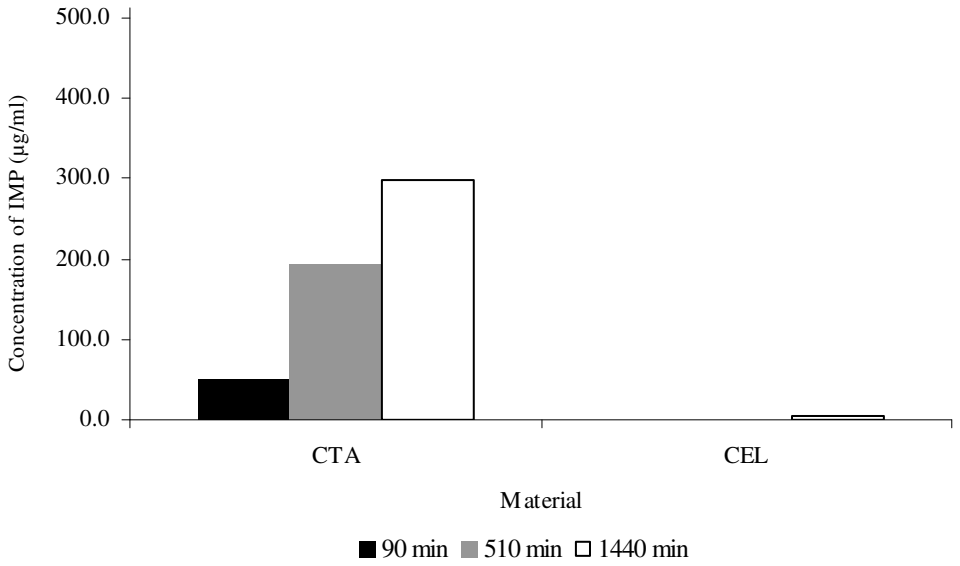

Figure 18 – Concentration of Imipenem (IMP) incorporated by cellulose triacetate (CTA) and cellophane (CEL) along the time of the experiment.

The concentration of Imipenem at 90 min (black bars), at 510 min (grey bars) and at 1440 min (white bars), after incorporation in each material, can be observed in Fig. 18. The data presented in this figure represents the IMP concentration adsorbed by the disk, taking into account the amount of antibiotic adsorbed by the flasks (initial concentration: 512 µg/ml). As can be observed CTA was the material incorporating the highest amount of IMP and the incorporation of IMP increased with time. Although CTA was the material with higher incorporation after 1440 min these results can be misleading because of the CTA altered structure. The rough surface morphology may be explained by the rapid evaporation of acetone. In fact, these CTA membranes were considered inadequate for further bacterial adhesion studies and therefore the use of acetone was replaced by chloroform-methanol as a solvent for CTA .

3.3.3. IMP release studies

CTA-IMP and CEL disks were immersed in saline solution and removed throughout the time of the experiment. The solutions were measured using UV spectroscopy at 298 nm (Fig. 19).

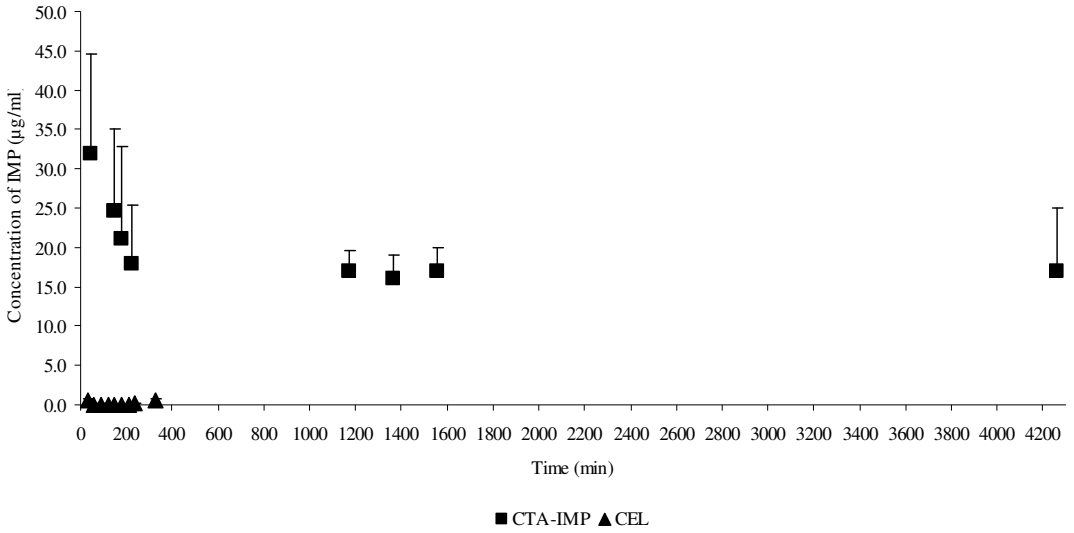

Figure 19 - Concentration of IMP incorporated by CTA-IMP and CEL.

The concentrations of Fig. 19 were calculated from the eq. 14. Fig. 19 illustrates the amount of IMP released by CTA-IMP and CEL measured at 298 nm. In the case of CEL almost no antibiotic was released, as a consequence of the low incorporation (Fig. 18). Samples were taken until stabilization of the amount of antibiotic released. Samples for release studies from CEL were taken during 330 min. In the case of CTA stabilization ocuured much later in time. Fig. 19 shows a gradual decrease in the IMP released from CTA until 1365 min, after which there was a stabilization in the release values until 4260 min. According to Venditti et al. (1999) or Yigong et al. (2004) the concentration of IMP during whole the release assay was supra-MIC. Therefore, the IMP concentration near the surface is certainly bactericidal, thus avoiding the selection of resistance strains. This data confirms CTA as an adequate reservoir for IMP entrapment and its subsequent sustained release over an appropriate period of time at an effective concentration. Furthermore, even when bacteria are still not near the material surface they can be affected by MICs or sub-MICs of antibiotic. In the latter case, as described by Martinez-Martinez et al. (1991), bacteria can be affected in their adhesion abilities.

3.4. Bacterial adhesion

3.4.1. Surface free energy determination between strains, surface adhesion and water

Table 10 shows the values of the surface free energy of interaction between bacterial and materials' surfaces and water. A value of ΔG_{bws}^{TOT} positive means that adhesion is not thermodinamically possible or viable, which occurs when the bacteria adhere to CTA and CTA-IMP disks. If the ΔG_{bws}^{TOT} value is negative it means that the adhesion of bacteria to the material surface is thermodinamically favored; that is, the more negative the value of ΔG_{bws}^{TOT} the higher will be the number of adhered cells.

Table 10 – Values of the surface free energy of interaction between the materials, *S. epidermidis* and water.

Material/Strain	ΔG_{bws}^{LW} (mJ/m2)	ΔG_{bws}^{AB} (mJ/m2)	ΔG_{bws}^{TOT} (mJ/m^2)
Material in contact with			
RP62A			
CTA	-1.28	12.91	11.63
CTA-IMP	-1.31	23.64	22.33
Strain in contact with CTA			
RP62A	-1.28	12.91	11.63
M187-Sn3	-3.38	12.24	8.86

In the present work, the adhesion assays were carried out in a saline solution (pH = 7.0). In this case the thermodynamic analysis becomes increasingly important given that the bacteria behave as "live coloids". Data presented in Table 10 shows that the presence of IMP on CTA membranes increased the ΔG_{bws}^{TOT} value, thus enabling a decrease in the available energy for adhesion. Table 10 also shows the differences in ΔG_{bws}^{TOT} values for capsulated and non-capsulated bacteria adhering to CTA. As can be observed there are no significant differences between strains with different phenotypes.

3.4.2. Adhesion assay

Fig. 20 represents the Optical Density (OD) values of adhesion of *S. epidermidis* RP62A and M187-Sn3 to polystyrene of 24-well microtitre plates.

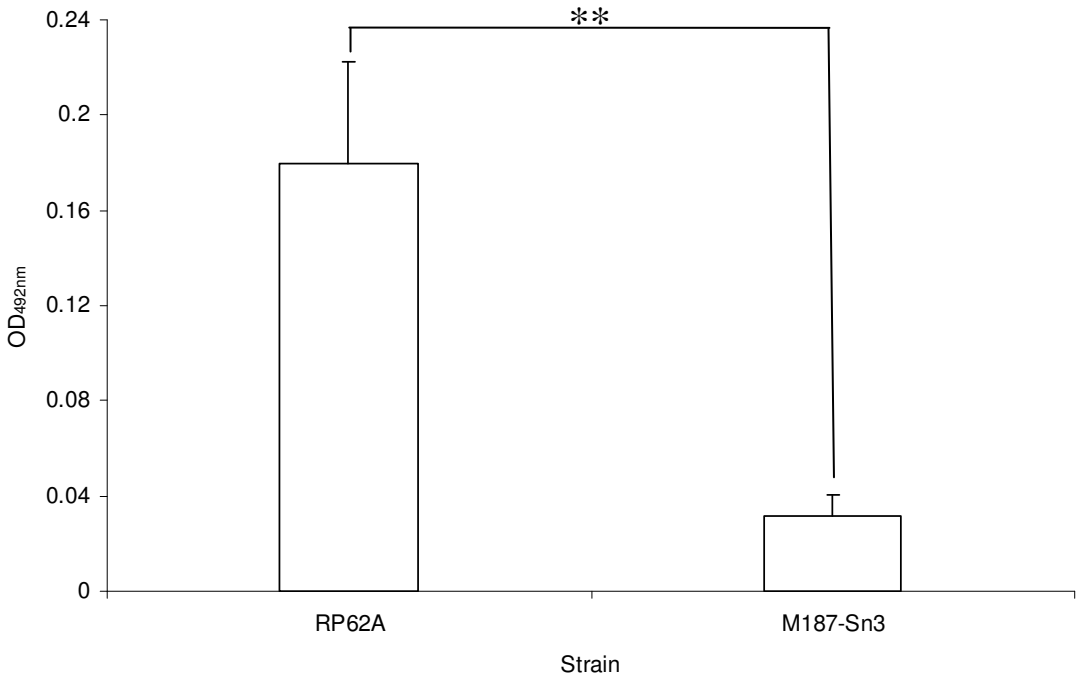

Figure 20 - Comparison between adhesion of *S. epidermidis* RP62A and M187-Sn3 to polystyrene. ** Represents a mean difference significant at the P <0.01 level (paired sample *t*-test test).

As can be seen in the Fig. 20 there are statistically significant differences between the adhesion of PS/A$^+$ RP62A and the PS/A$^-$ M187-Sn3 to PS, allowing to select RP62A for further adhesion studies as representative of strains with high adhesion values. *S. epidermidis* RP62A is less hydrophilic than M187-Sn3 (Table 6), and as a consequence it is expected to present higher adhesion values to hydrophobic surfaces, namely the polystyrene of microtitre plates (Tresse et al., 2006). This polystyrene (hydrophobic) was not the same as the polystyrene disks (hydrophilic) previously studied in this work.

Fig. 21 shows the difference between *S. epidermidis* RP62A adhesion to unmodified cellulose triacetate disks (CTA) and to cellulose triacetate and Imipenem disks (CTA-IMP).

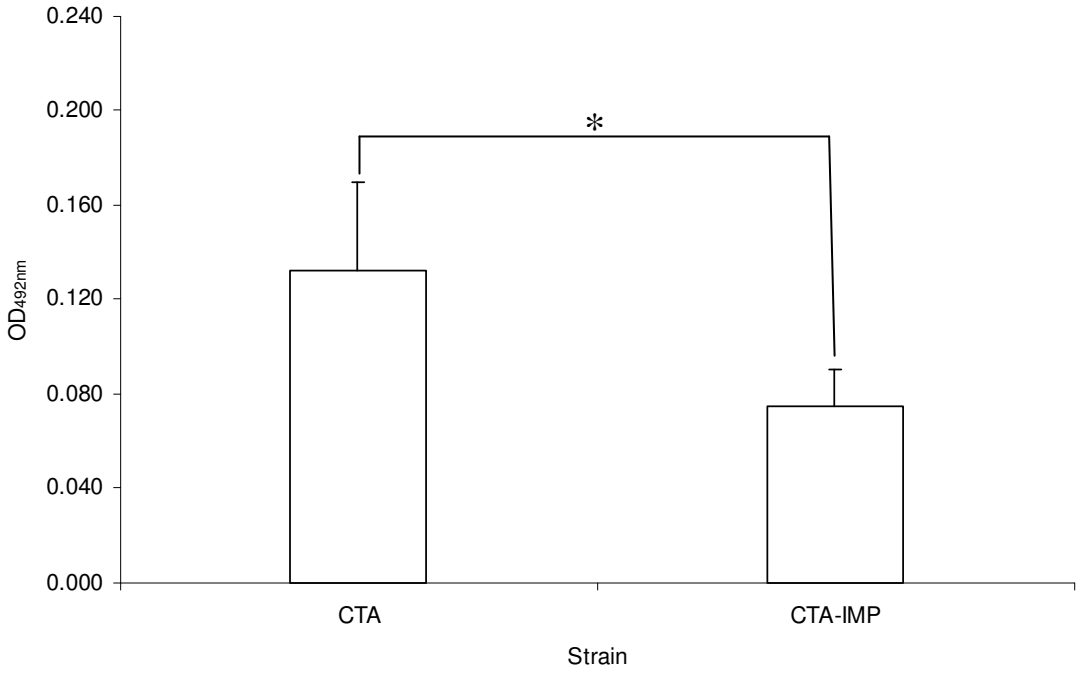

Figure 21 - Comparison between *S. epidermidis* RP62A adhesion to CTA and CTA-IMP. * Represents a mean difference significant at the P <0.05 level (paired sample *t*-test test).

Fig. 21 shows a significant decrease (P <0.05) in the adhesion of *S. epidermidis* RP62A to CTA-IMP when compared to its adhesion to CTA. These results can be explained by the fact that the presence of the antibiotic on the material turns it hydrophilic (Table 9). The adhesion between *S. epidermidis* RP62A and CTA and CTA-IMP is not thermodynamically favoured since the total free energy of interaction between the bacteria, material and water is positive (Table 9). Nevertheless, the free energy of interaction ΔG_{bws}^{TOT} is more positive for CTA-IMP, thus making it the surface with less energy available for the occurrence of adhesion. The presence of a significant amount of antibiotic released from the material during 2 h of the adhesion assay (Fig. 19) may kill or affect the adhesion ability of the *S. epidermidis* strain. Martinez-Martinez et al. (1991) found that sub-inhibitory concentrations of beta-lactams affect the production of

slime, the surface hydrophobicity and the adhesion od of *S. epidermidis*. These findings may also explain the reduction in adhesion ability of the strain studied in the presence of IMP released from CTA membranes.

3.4.3. Kirby Bauer test

Fig. 22 shows the inhibition zones of *S. epidermidis* RP62A after growing in presence of CTA or CTA-IMP membranes.

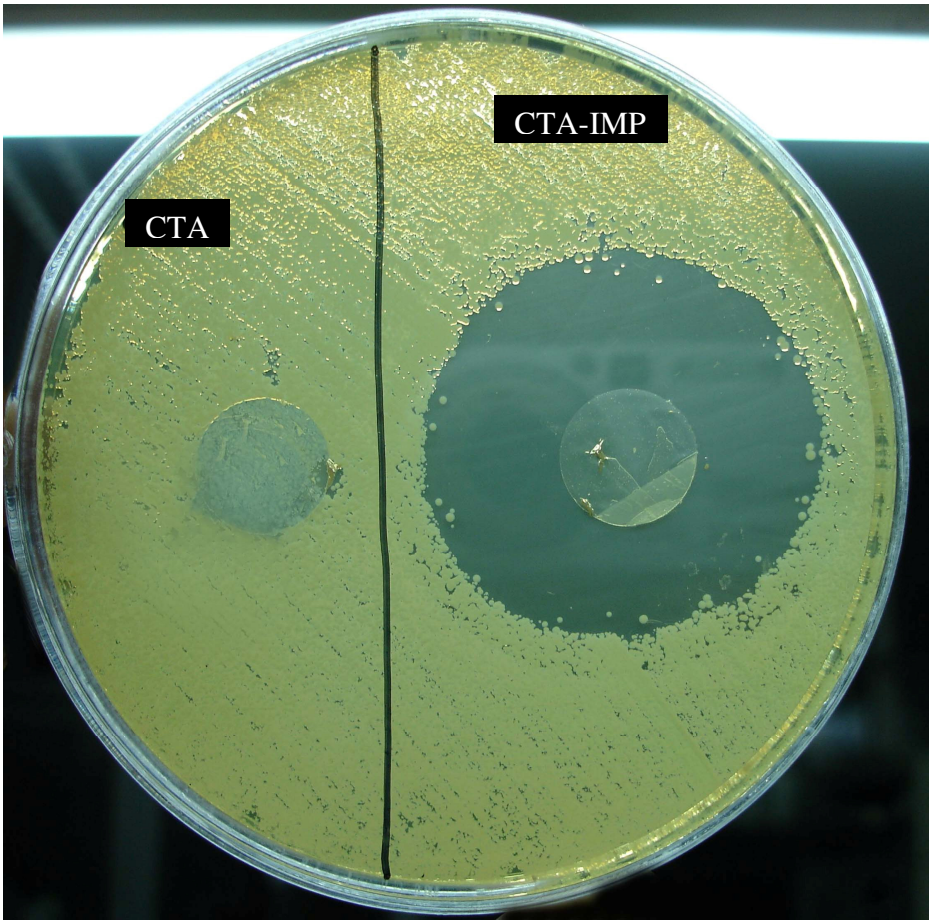

Figure 22 – Bacterial inhibition zone performed by Kirby Bauer test for CTA and CTA-IMP.

As is ilustrated in Fig. 22 there was no inhibition zone caused by the CTA disk, which was expected as this material does not have an inhibitory effect "per se", neither incorporates the antibiotic IMP. On the other hand, an inhibition zone is evident on the right side of Fig. 22, caused by the IMP entraped on the CTA disk. These results

indicate that IMP is functional after the entrapment on the CTA membrane. It is thus shown that CTA-IMP membranes have an anti-proliferative character, being therefore bacteriostatic.

Figs. 23 through 26 show SEM micrographs of the membranes with *S. epidermidis* RP62A adhered after the adhesion assay.

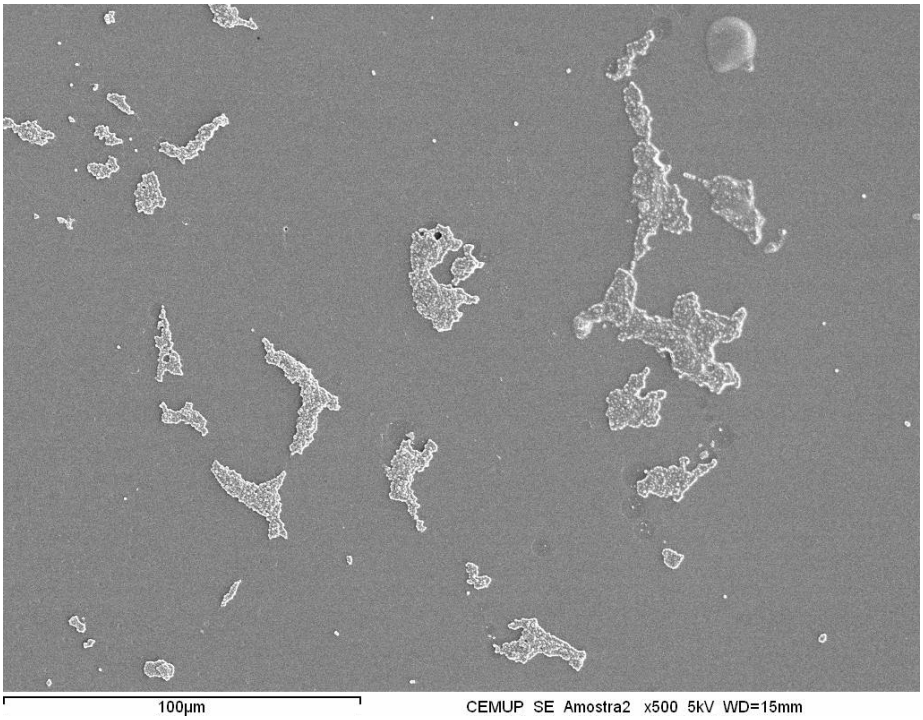

Figure 23 – SEM micrograph of RP62A strain adhered to a CTA disk.

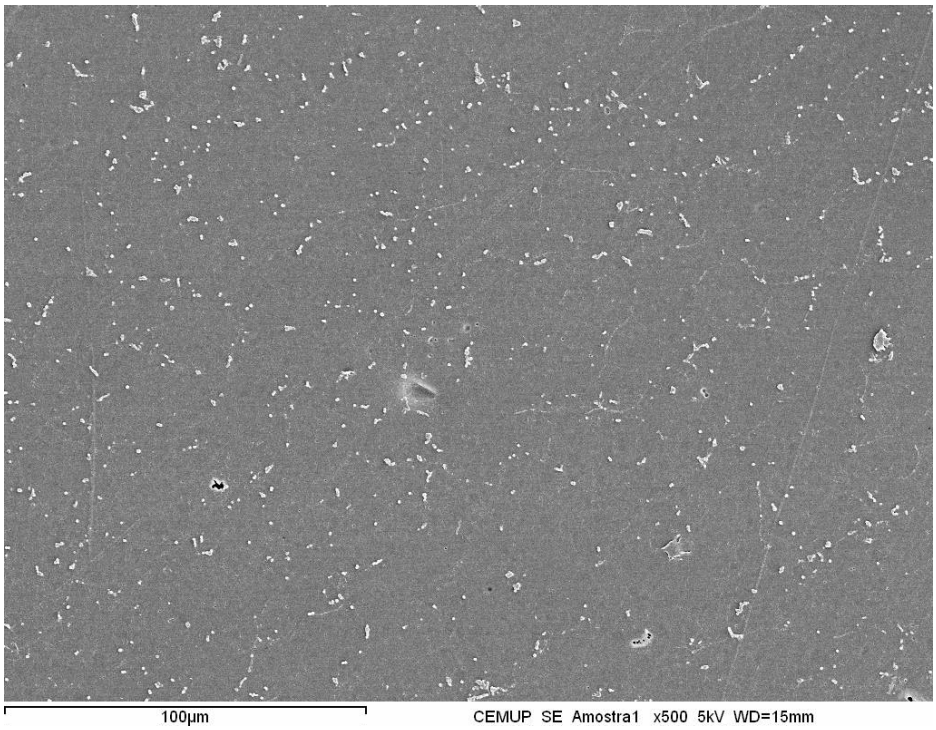

Figure 24 – SEM micrograph of RP62A strain adhered to a CTA-IMP disk.

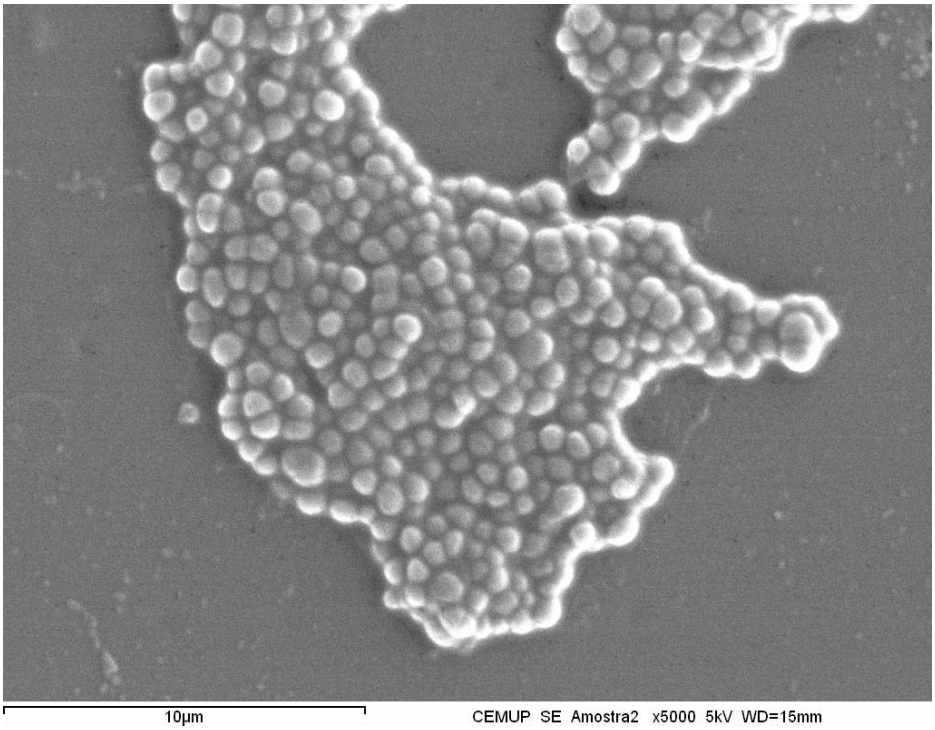

Figure 25 – SEM micrograph of RP62A strain adhered to a CTA disk.

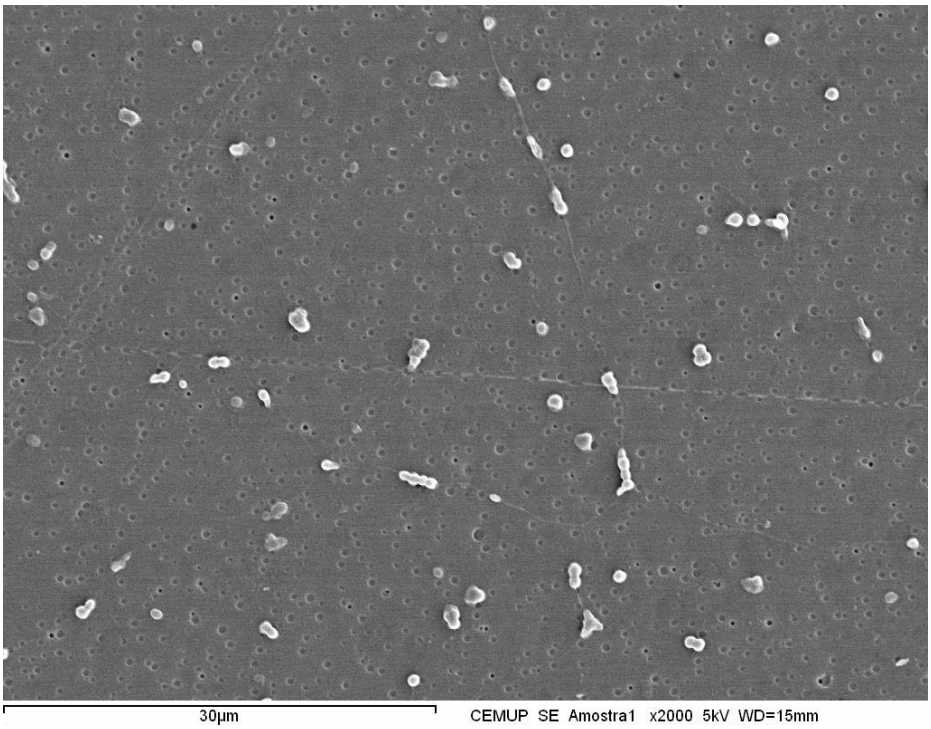

Figure 26 – SEM micrograph of RP62A strain adhered to a CTA-IMP disk.

Figs. 23 through 26 illustrate the bacterial adhesion pattern on the CTA surface and a minor adhesion to the material incorporating the antibiotic (CTA-IMP), which is in accordance with the values obtained in the adhesion assay. Figs 23 and 25 show that RP62A formed microcolonies. The formation of aggregates can be seen in the membrane's surface. From the thermodynamic approach it was observed that CTA is an hydrophobic surface, therefore promoting a higher adhesion of a less hydrophilic strain. Figs 24 and 25 show a considerably lower adhesion and that the strains are more spread at the CTA-IMP membrane. This can be possibly explained by the hydrophilicity of the surface caused by the IMP entrapment, in conjunction with the effect of IMP itself released during the process of adhesion, as well as by the change in surface morphology caused by the entrapment of IMP (the "nanoholes" observed in Fig. 26). In Fig. 25 it can be observed that there was no alteration on the CTA membrane surface.

3.5. Importance of the thermodynamic approach on bacterial adhesion to surfaces

One of the purposes of the present work was to use a thermodynamic approach to understand or explain the behaviour of bacteria interacting with material's surfaces. The contact angle measurements of bacteria and material surfaces enable the calculation of the respective surface tensions, the free energy of interaction between the surfaces and water (quantitative measure of hydrophobicity) and the free energy of interaction between bacteria, water and material surface.

There are no consensus in the literature concerning the way to calculate surface tension and free energy of interaction, namely in complex systems involving bacteria. According to Morra and Cassinelli (1997), the heterogeneity of the surfaces cannot be measured at the micro ou submicrometer level by contact angle measurements, and thus the data could be misleading in the calculation of free energy of interaction.

Several studies are available concerning the correlation between a thermodynamic approach and bacterial adhesion. Morra and Cassinelli (1996) described that *S. epidermidis* adhered more with the decrease of the free energy of interaction; Fonseca et al. (2001) reported similar findings for the adhesion to cellulose diacetate. Jansen and Kohnen (1995) and Fonseca et al. (2001) described a correlation between the free energy of interaction between bacteria, water and material surface and bacterial adhesion values, thus concluding that the adhesion is thermodynamically favoured when the energy of interaction is negative. Nevertheless, the increase of material hydrophilicity does not avoid bacterial adhesion, since there are always bacteria adhering to the surface, as was confirmed by the present results.

The reasons for some contradictory data in the literature are related, for instance, with the use of different strains or media or even the fact that the adhesion assays can be static or dynamic (Cristensen et al., 1995). Furthermore, there are several different approaches to calculate the surface free energy and the energies of interaction. In the present work the Good-van Oss-Chaudory approach was used (van Oss et al., 1987), as suggested by Morra and Cassinelli (1997), that allows the calculation of the LW and the electron acceptor and electron donor parameters of the surfaces, through a system of three equations and three unknowns. In this case, at least three liquids are required. In the present work, higher γ^- values comparing to the γ^+ values were obtained for CTA, which is in accordance with previously reported work for CDA (Fonseca et al., 2001)

and CA (van Oss et al., 1987). The present results confirm the importance of the γ^- in the quantitative measurement of hydrophobicity and subsequently in the calculation of the free energy of interaction between bacteria, water and material surfaces.

3.6. Influence of the surface properties of the materials and bacteria

There are several factors affecting bacterial adhesion, namely rugosity, charge, surface chemical composition, surface morphology and hydrophobicity. The present results confirm that the adsorption and/or incorporation of an antibiotic in a biomaterial can change its surface properties, namely decreasing material hydrophobicity, in the case of hydrophobic materials (silicone and PVC). This decrease in hydrophobicity was also observed for the hydrophobic CTA; in this case the antibiotic changed the material surface from hydrophobic to hydrophilic. These changes in the material surface properties can explain the significant decrease in bacterial adhesion, confirming previous reports from Ludwicka et al. (1984) and, more recently, from Fonseca et al. (2001; 1999). They concluded that more hydrophilic materials are more resistant to bacterial adhesion comparing to hydrophobic materials.

Locci et al. (1981) described that materials' surface irregularities increase bacterial adhesion. In our case, although there was a change in CTA surface morphology (as observed by SEM) after the incorporation of Imipenem promoted even a significant decrease in the bacterial adhesion values. However, no correlation to surface roughness was attempted since the chemical characteristics of the surface were changed.

The measurements of the contact angles on bacteria allow the quantification of hydrophobicity. Present results confirm the importance of the presence of PS/A as a mediator in bacterial adhesion to polystyrene, namely by the significantly higher adhesion values for strain PS/A+ RP62A comparing to the PS/A – M187-Sn3 (Fonseca, 1999).

4. Conclusions and Perspectives

The main purpose of the present work was to develop strategies to coat medical devices, providing the release of an antibiotic while maintaining the bulk properties of the material. The preparation of CTA membranes with entrapped Imipenem (CTA-IMP) was effective using chloroform-methanol as solvent. Entrapped Imipenem increased the hydrophilicity of CTA membranes. The present approach provided a sustained release of Imipenem over an adequate period of time (at least 71h) at an effective bacteriostatic concentration. The Kirby Bauer test further demonstrated that CTA-IMP has anti-proliferative properties and a bacteriostatic effect in bacteria. By using the present approach it seems possible to obtain an adequate medical device surface coated with CTA-IMP with anti-adhesive and anti-proliferative properties.
Surface and interfacial energy on the adhesion of *S. epidermidis* RP62A to biomaterials presented a good correlation between the thermodynamic approach and experimental data.

The perspectives of the present work are:

- Development of an effective coating technology of CTA-IMP on the surface of biomedical polymers by surface modification of the substrate;
- Entrapment of IMP at different concentrations on CTA membranes and assessment of its influence on bacterial adhesion;
- Study the process of antibiotic release and adhesion in dynamic conditions;
- Investigation of the influence of CTA-IMP membranes on the adhesion of clinical isolates of *S. epidermidis*.

5. References

Ahlberg A, Carlsson AS, Lindberg L. Hematogenous infection in total joint replacement. Clin Orthop Relat Res 1978; 137: 69-75.

Akiyama H, Okamoto S. Prophylaxis of indwelling urethral catheter infection: clinical experience with a modified Foley catheter and drainage system. J Urology 1979; 121: 40-42.

Aldridge KE, Ashcraft D, O'Brien M, Sanders CV. Bacteremia due to *Bacteroides fragilis* Group: Distribution of Species, β-Lactamase Production, and Antimicrobial Susceptibility Patterns. Antimicrob Agents Chemother 2003; 47 (1): 148-153.

An YH, Friedman RJ. Concise review of mechanisms of bacterial adhesion to biomaterial surfaces. J Biomed Mat Res 1998; 43: 338-348.

Andrade JD, Smith LM, Gregonis DE. The contact angle and interface energetics. In: Surface and Interfacial Aspects of Biomedical Polymers. Andrade JD, editor. New York: Plenum Press 1985. 249-292.

Arciola CR, Campoccia D, Montanaro L. Effects on antibiotic resistance of *Staphylococcus epidermidis* following adhesion to polymethylmethacrylate and to silicone surfaces. Biomaterials 2002; 23(6):1495-502.

Asaria RH, Downie JA, McLauglin-Borlace L, Morlet N, Munro P, Charteris DG. Biofilm on scleral explants with and without clinical infection. Retina 1999; 19: 447-450.

Balazs DJ, Triandafillu K, Wood P, Chevolot Y, van Delden C, Harms H, Hollensteind C, Mathieua HJ. Inhibition of bacterial adhesion on PVC endotracheal tubes by RF-oxygen glow discharge, sodium hydroxide and silver nitrate treatments. Biomaterials 2004; 25: 2139-2151.

Beamson G and Briggs D, editors. High Resolution XPS of Organic Polymers – The Scienta ESCA300 Database. John Wiley & Sons Ltd. Chichester, England. 1992.

Bengtson S, Blomgren G, Knutson K, Wigren A, Lidgren L. Hematogenous infection after knee arthroplasty. Acta Orthop Scandin 1987; 58: 529-34.

Bhat NV, Wavhal DS. Preparation of cellulose triacetate pervaporation membrane by ammonia plasma treatment. J Applied Polymer Science 2000; 76: 258-265.

Bridgett MJ, Davies MC, Denyer SP. Control of staphylococcal adhesion to polystyrene surfaces by polymer surface modification with surfactants. Biomaterials 1992; 13: 111-116.

Brisset L, Vernet-Garnier V, Carquin J, Burde A, Flament JB, Choisy C. In vivo and in vitro analysis of the ability of urinary catheter to microbial colonization. Pathol Biol 1996; 44: 397-404.

Bridgett MJ, Davies MC, Denyer SP. Control of staphylococcal adhesion to polystyrene surfaces by polymer surface modification with surfactants. Biomaterials 1992; 13: 411-416.

Busscher HJ, Weerkamp AH. Specific and non-specific interactions in bacterial adhesion to solid substrata. FEMS Microb Rev 1987; 46: 165-173.

Calderwood SB, Swinski LA, Waternaux CM. Risk factors for the development of prosthetic valve endocarditis. Circulation 1985; 72: 31-37.

Carlsson AS, Josefsson G, Lindberg L. Revision with gentamicin-impregnated cement for deep infections in total hip arthroplasties. J Bone Joint Surg 1978; 60: 1059-1064.

Charnley J. Postoperative infection after total hip replacement with special reference to air contamination in the operating room. Clin Orthop Relat Res 1972; 87: 167-187.

Christensen GD, Baddour LM, Hasty DL, Lowrance JH Simpson WA. Microbial and foreign body factors in the pathogenesis of medical device infections. In: Infections associated with indwelling medical devices. Bisno AL, Waldvogel FA, editors. American Society of Microbiology. Washington DC 1989. 27-59.

Christensen GD, Baldassami L, Simpson WA. Methods for studying microbial colonisation of plastics. In: Adhesion of microbial pathogens. Methods in Enzymology. Doyle RJ, Oftek I, editors. Academic Press Inc. San Diego 1995. 447-500.

Cooksey K. Effectiveness of antimicrobial food packaging materials. Food Addit Contam 2005; 22 (10): 980-987

Costerton JW, Ellis B, Lam K, Johnson F, Khoury AE. Mechanism of electrical enhancement of efficacy of antibiotics in killing biofilm bacteria. Antimicrob Agents Chemother 1994; 38: 2803-9.

Costerton JW, Stewart PS, Greenberg EP. Bacterial biofilms: a common cause of persistent infections. Science 1999; 284: 1318-1322.

Dankert J, Hogt AH, Feijen J. Biomedical polymers: Bacterial adhesion, colonization and infection. CRC Critical Reviews in Biocompatibility 1986; 2: 219-301.

Della Volpe C, Siboni S. Some reflections on acid-base solid surface free energy theories. J Coll Interf Science 1997; 195: 121-136.

Demirer S, Geçim IE, Aydınuraz K, Ataoglu H, Yerdel MA, Kuterdem E. Afinity of *Staphylococcus epidermidis* to various prosthetic graft materials. J Surgical Research 2001; 99: 70-74.

Denstedt JD, Wollin TA Reid G. Biomaterials used in urology: current issues of biocompatibility, infection, and encrustation. J Endourology 1998; 12: 493-500.

Donelli G, Francolini I, Piozzi A, Di Rosa R, Marconi W. New polymer-antibiotic systems to inhibit bacterial biofilm formation: a suitable approach to prevent central venous catheter-associated infections. J Chemother 2002; 14 (5): 501-507.

Duran L, Driemeyer JE, Jelle BM, Jenderko JA, Muggli ME, Sitarz KE, Daws KM. Surface Modification to reduce urinary catheter infection. Surfaces in Biomaterials: Symposium Note-book 1995; 45.

Elam JH, Elam M. Surface modification of intravenous catheters to reduce local tissue reactions. Biomaterials 1993; 14 (11): 861-864.

Elam JH, Karlsson CH, Nygren H. Pre-adsorption of cellulose ether onto polymer surfaces: adsorption of adhesins and platelet activation. Biomaterials 1992; 14 (3): 233-237.

Elek SD, Conen PE. The virulence of *Staphylococcus pyogenes* for man. A study of the problems of wound infection. Brit J Exp Pat 1957; 38: 573-586.

Everaert EP, Mahieu HF, Van de Belt-Gritter B, Peeters AJ, Verkerke GJ, Van der Mei HC, Busscher HJ. Biofilm formation in vivo on perfluoro-alkylsiloxane-modified voice prostheses. Archiv Otolaryngo: Head Neck Surg 1999; 125: 1329-32.

Fisch A, Salvanet A, Prazuk T. Epidemiology of infective endophthalmitis in France. The French collaborative study group on endophthalmitis. Lancet 1991; 338: 1373-1376.

Fitzgerald RH, Jones DR. Hip implant infection. Treatment with resection arthroplasty and late total hip arthroplasty. Amer J Med 1985; 78: 225-228.

Flemming RG, Capelli CC, Cooper SL, Proctor RA. Bacterial colonization of functionalized polyurethanes. Biomaterials 2000; 21: 273-281.

Fonseca AP. Adesão de *S. epidermidis* a biomateriais poliméricos. FEUP, editors. Porto, Portugal. 1999.

Fonseca AP, Granja PL, Nogueira JA, Oliveira DR, Barbosa MA. *Staphylococcus epidermidis* RP62A adhesion to chemically modified cellulose derivatives. J Mats Sci: Mats Med 2001; 12: 543-548

Fonseca AP, Extremina C, Fonseca AF, Sousa JC. Effect of subinhibitory concentration of piperacillin/tazobactam on *Pseudomonas aeruginosa*. J Med Microbiol 2004; 53: 903-910.

Freeman DJ, Falkiner FR, Keane CT. New method for detecting slime production by coagulase negative staphylococci. J Clin Pathol 1989; 42: 87-874.

Gilbert P, Das J, Foley I. Biofilm susceptibility to antimicrobials. Adv Dent Res 1997; 11: 160-167.

Granja PL, Baquey C, Pouységu L, Bareille R, De Jéso B, Barbosa MA. Cellulose-based biomaterials for bone regeneration: Hemi-synthesis and characterisation. Polymers in Medicine and Surgery 1996; PIMS'96. Glasgow, United Kingdom:73-80.

Gristina AG. Biomaterial-centered infection: microbial adhesion versus tissue integration. Science 1987; 237: 1588-1595.

Gross M, Cramton SE, Gotz F, Peschel A. Key role of teichoic acid net charge in *Staphylococcus aureus* colonization of artificial surfaces. Infect Immun 2001; 69: 3423-3426.

Gottenbos B. The development of antimicrobial biomaterial surfaces. Faculty of Medical Sciences, editors. Groningham, Netherlands 2001. 9-24.

Hogt AH, Dankert TJ, De Vries JA, Feijen J. Adhesion of coagulase-negative *Staphylococci* to biomaterials. J Gen Microbiol 1983; 129: 2959-2968.

Hogt AH, Dankert TJ, Feijen J. Adhesion of *Staphylococcus epidermidis* and *Staphylococcus saprophyticus* onto a hydrophobic biomaterial. J Gen Microbiol 1985; 131: 2485-2491.

Hogt AH, Dankert TJ, Hulstaert CE, Feijen J. Cell surface characteristics of coagulase negative staphylococci and their adherence to fluorinated poly (ethylenepropylene). Infect Immun 1986; 51: 294-301.

Hunter G, Dandy D. The natural history of the patient with an infected total hip replacement. J Bone Joint Surg Br 1977; 59(3): 293-297.

Ishizu A. Chemical modification of cellulose. In: Wood Cellul. Chem, D.N.-S. Hon editors. 1991. 757-800.

Ista LK, Fan H, Baca O, Lopez GP. Attachment of bacteria to model solid surfaces: oligo (ethylene glycol) surfaces inhibit bacterial attachment. FEMS Microb Letters 1996; 142: 59-63.

Jacqueline C, Navas D, Batard E, Miegeville AF, Le Mabecque V, Kergueris MF, Bugnon D, Potel G, Caillon J. In vitro and in vivo synergistic activities of linezolid combined with subinhibitory concentrations of imipenem against methicillin-resistant *Staphylococcus aureus*. Antimicrob Agents Chemother 2005; 49(1): 45-51.

Jansen B, Kohnen W. Prevention of biofilm formation by polymer modification. J Indust Microb 1995; 15: 391-396.

Kenawy E, Abdel-Hay FI, El-Shanshoury AR, El-Newehy MH. Biologically active polymers: synthesis and antimicrobial activity of modified glycidyl methacrylate polymers having a quaternary ammonium and phosphonium groups. J Control Release 1998; 50: 145-152.

Keogh JR, Eaton JW. Albumin binding surfaces for biomaterials. J Lab Clin Med 1994; 124: 537-45.

Kishida A, Mishima K, Corretge E, Konishi H, Ikada Y. Interactions of poly(ethylene glycol)grafted cellulose membranes with proteins and platelets. Biomaterials 1992; 13 (2): 113-118.

Klem L, Philipp B, Heinze T, Wagenknecht W. Comprehensive Cellulose Chemistry, Vol. 1. Fundamentals and Analytical Methods.Wiley-VCH, Weinheim, Germany. 1998.

Klotz SA, Drutz DS, Zajic JE. Factors governing adherence of *Candida* species to plastic surfaces. Infect Immun 1985; 50: 97-101.

Lidwell OM, Lowbury EJ, Whyte W, Blowers R, Stanley SJ, Lowe D. Effect of ultraclean air in operating rooms on deep sepsis in the joint after total hip or knee replacement: a randomised study. Brit Med J Clin Res Edition 1982; 285: 10-14.

Liedberg H, Lundeberg T. Assessment of silver-coated urinary catheter toxicity by cell culture. Urol Res 1989; 17: 357-360.

Locci R, Peters G, Pulverer G. Microbial colonisation of prosthetic devices. 1. Microtopographical characteristics of intravenous catheters as detected by scanning electron microscopy. Zbl Bakt Hyg I Abt Orig B 1981; 173: 285-292.

Ludwicka A, Jansen B, Wadstrom T, Pulverer G. Attachment of *staphylococci* to various synthetic polymers. Zbl Bakt Hyg 1984; A256: 479-489.

Mahieu HF, Saene HF, Rosingh HJ, Schutte HK. Candida vegetations on silicone voice prosthesis. Arch Otolaryng 1986; 112: 321-325.

Maki DG, Weise CE, Sarafin HW. A semiquantitative culture method for identifying intravenous-catheter-related infection. J. Med 1977; 296: 1305-1308.

Maniloff G, Greenwald R, Laskin R, Singer C. Delayed post bacteremic prosthetic joint infection. Clin Orthop Relat Res 1987; 223: 194-197.

Martinez-Martinez L, Pascual A, Giglio MI, Perea EJ. Effect of subinhibitory concentrations of beta-lactams on the production of slime, surface hydrophobicity and adhesion of *Staphylococcus epidermidis*. 1991; 9 (9): 543-546.

Mayer KH, Schoenbaum SC. Evaluation and management of prosthetic valve endocarditis. Progr Cardiov Dis 1982; 25: 43-54.

Mayhall CG, Archer NH, Lamb A.Ventriculostomy-related infections: a prospective epidemiologic study. N Eng J Med 1982; 310: 553-559.

Morra M, Cassinelli C. *Staphylococcus epidermidis* adhesion to films deposited from hydroxyethylmethacrylate plasma. J Biomat Res 1996; 31 (2): 149-156.

Morra M, Cassinelli C. Bacterial adhesion to polymer surfaces: a critical review of surface thermodynamic approaches. J Biomat Sci 1997; Polymer Edition, 9 (1): 55-74.

Muller E, Hubner J, Gutierrez N, Takeda S, Goldmann DA, Pier GB. Isolation and characterization of transposon mutants of *Staphylococcus epidermidis* deficient in capsular polysaccharide/adhesin and slime. Infect Immun 1993; 61: 551-558.

Nickel JC, Costerton JW, McLean RJ, Olson M. Bacterial biofilms: influence on the pathogenesis, diagnosis and treatment of urinary tract infections. J Antimicrob Chemother 1994; supplement A 33: 31-41.

Okada K, Yokogawa Y, Kameyama T, Kato K, Kawamoto Y, Nishizawa K, Nagata F, Okuyama M. Antibacterial property of Ag-doped calcium phosphate compound-cellulose composites. Bioceramics 1997; 10: 329-332.

Ono S, Muratani T, Matsumoto T. Mechanisms of Resistance to Imipenem and Ampicillin in *Enterococcus faecalis*. Antimicrob Agents Chemother 2005; 49(7): 2954-2958.

O'Toole GA, Pratt LA, Watnick PI, Newman DK, Weaver VB, Kolter R. Genetic approaches to study of biofilms. Methods Enzymol 1999; 310: 91-105.

Owens DK, Wendt RC. Estimation of the surface free energy of polymers. J Appl Polym Sci 1969; 13:1741-1747.

Pascual A. Pathogenesis of catheter-related infections: lessons for new designs. Clin Microbiol Infect 2002; 8: 256-264.

Pearson ML, Abrutyn E. Reducing the risk for catheter-related infections: a new strategy. Ann Intern Med 1997; 127: 304-306.

Rad YA, Ayhan H, Piskin E. Adhesion of different bacterial strains to low-temperature plasma-treated sutures. Wiley & Sons, J Biomed Mater Res 1998; 41: 349-358.

Ratner BD. New ideas in biomaterials science – A path to engineered biomaterials. J Biomed Mat Res 1993; 27: 837-850.

Rediske AM, Roeder BL, Brown MK, Nelson JL, Robison RL, Draper DO, Schaalje GB, Robison RA, Pitt WG. Ultrasonic enhancement of antibiotic action on *Escherichia coli* biofilms: an in vivo model. Antimicrob Agents Chemother 1999; 43: 1211-4.

Rosenberg E, Gottlieb A, Rosenberg M. Inhibition of bacterial adherence to hydrocarbons and epithelial cells by emulsan. Infect Immun 1983; 39: 1024-1028.

Schoenbaum SC, Gardner P, Shilito J. Infections of cerebrospinal fluid shunts: epidemiology, clinical manifestations, and therapy. J Infect Dis 1975; 131: 543-552.

Shintani H. Modification of medical device surface to attain anti-infection. Trends Biomater. Artif. Organs 2004; 18 (1): 1-8.

Thomas MJK, Ando DJ, editors. Ultraviolet and visible spectroscopy: analytical chemistry by open learning. West Sussex: John Wiley& Sons. 1996.

Tobgi RS, Samaranjake LP, MacFarlane TW. Adhesion of Candida albicans to buccal epithelial cells exposed to chlorhexidine. J Med Vet Mycol 1987; 25: 335-338.

Tresse O, Lebret V, Benezech T, Faille C. Comparative evaluation of adhesion, surface properties, and surface protein composition of *Listeria monocytogenes* strains after cultivation at constant pH of 5 and 7. J Applied Microb 2006; 0 (0).

Vacheethasanee K, Temenoff JS, Higashi JM, Gary A, Anderson JM, Bayston R, Marchant RE. Bacterial surface properties of clinically isolated *Staphylococcus epidermidis* strains determine adhesion on polyethylene. J Biomed Mater Res 1998; 42: 425-432.

Van de Belt H, Neut D, Van Horn J, Van der Mei HC, Schenk W, Busscher HJ. ...or not to treat?. Nature Med 1999; 5: 358-359.

Van Oss CJ, Chaudhury MK, Good RJ. Monopolar surfaces, advances in colloid and interface science. Elsevier Sci Pub 1987; 28: 35-64.

Van Oss CJ. The forces involved in bioadhesion to flat surfaces and particles – their determination and relative roles. Biofouling 1991; 4: 25-35.

Venditti M, Santini C, Serra P, Micozzi A, Gentile G, Martino P. Comparative in vitro activities of new fluorinated quinolones and other antibiotics against coagulase-negative **Staphylococcus** blood isolates from neutropenic patients, and relationship between susceptibility and slime production. Antimicrob Agents Chemother 1989; 33 (2): 209-211.

Weinstein RA, Kabins SA, Nathan C. Gentamicin-resistant staphylococci as hospital flora: epidemiology and resistant plasmids. J Infect Dis 1982; 145: 374-382.

West TE, Walshe JJ, Krol CP. Staphylococcal peritonitis in patients on continuous peritoneal dialysis. J Clin Microbiol 1986; 23: 809-812.

Yigong Ge, Wikler MA, Sahm DF, Blosser-Middleton RS, Karlowsky JA. In vitro antimicrobial activity of Doripenem, a new Carbapenem. Antimicrob Agents Chemother 2004; 48 (4): 1384-1396.

Zhang X, Whitbourne R, Richmond RD. Surface Treatment. Antiinfective coatings for indwelling medical devices. Medical Plastics and Biomaterials Magazine 1997; 16.

Zimmerli W, Lew PD, Waldvogel FA. Pathogenesis of foreign body infection. Evidence for a local granulocyte defect. J Clin Investig 1984; 73: 1191-200.

Zimmerli W, Waldvogel FA, Vaudaux , Nydegger UE. Pathogenesis of foreign body infection: description and characteristics of an animal model. J Infect Dis 1982; 146: 487-497.

http://www.msd-egypt.com

6. Annexes

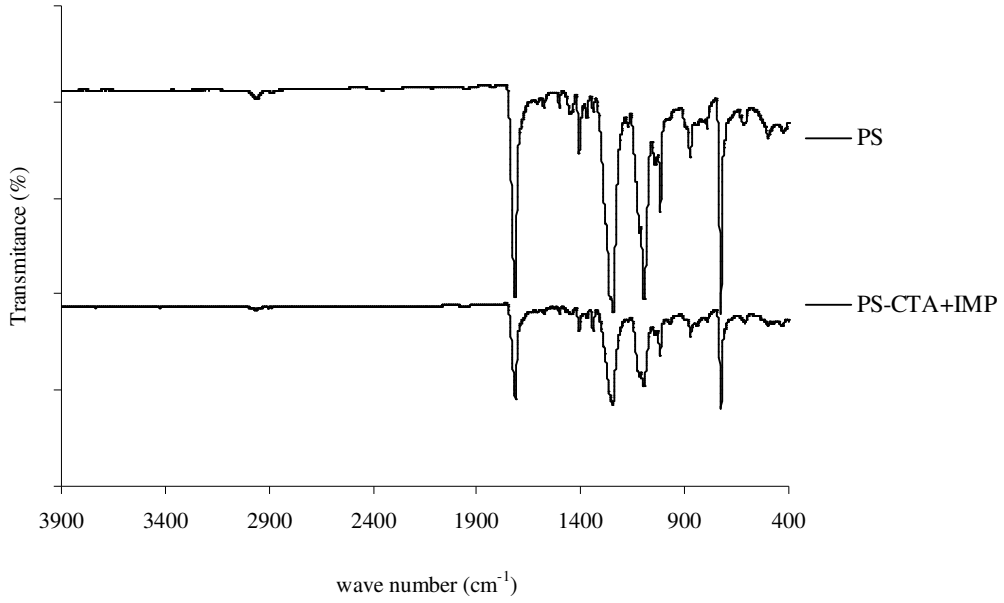

Figure 27 - ATR-FTIR spectrum of polystyrene (PS) and modified polystyrene with cellulose triacetate and Imipenem (CTA-IMP).

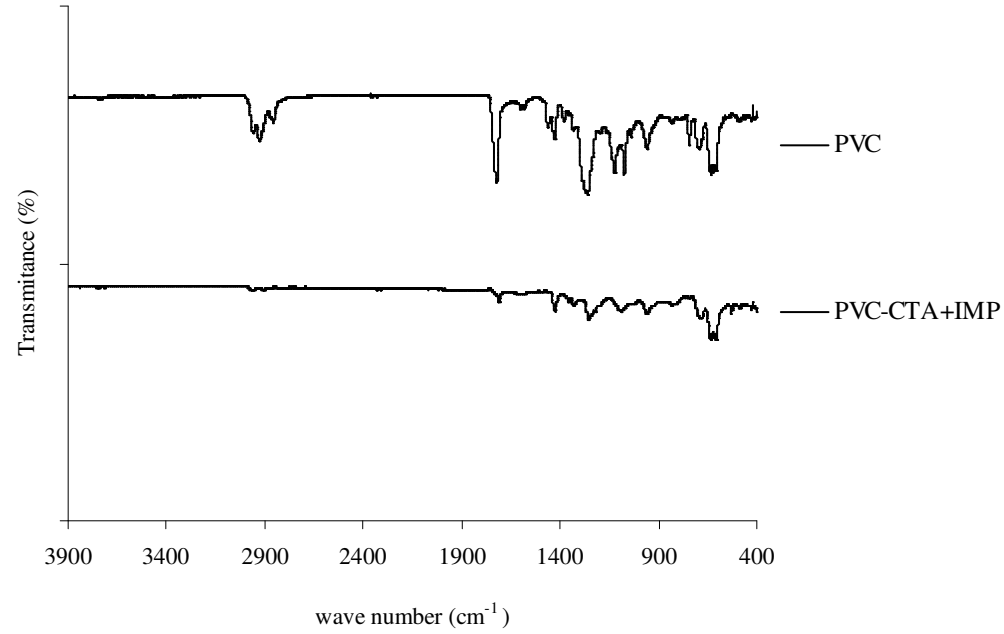

Figure 28 - ATR-FTIR spectrum of PVC and modified PVC with cellulose triacetate and Imipenem (PVC-CTA+IMP).

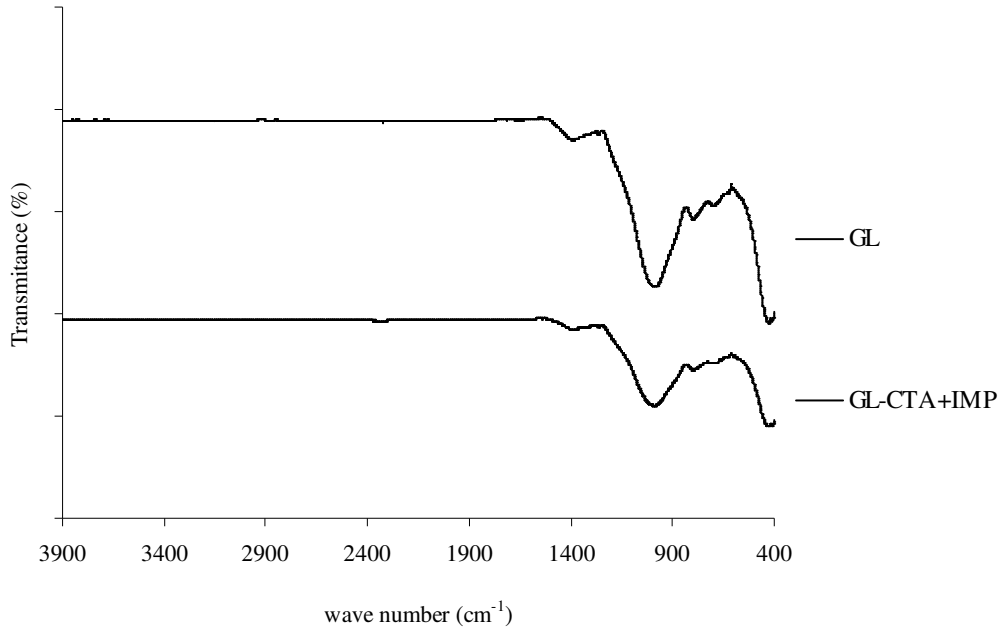

Figure 29 - ATR-FTIR spectrum of glass (GL) and modified glass with cellulose triacetate and Imipenem (GL-CTA+IMP).